Chem Soc Rev

Functional nucleic acid-based hydrogels for bioanalytical and biomedical applications

Journal:	*Chemical Society Reviews*
Manuscript ID	CS-SYN-07-2015-000586.R2
Article Type:	Review Article
Date Submitted by the Author:	09-Dec-2015
Complete List of Authors:	Li, Juan; Fuzhou University, College of Chemistry Mo, Liuting; Hunan University, Lu, Chun-Hua; Fuzhou University, College of Chemistry and Chemical Engineering Fu, Ting; Hunan university, chemistry Yang, HH; Fuzhou University, Tan, Weihong; P.O Box 117200, University of Florida

Functional nucleic acid-based hydrogels for bioanalytical and biomedical applications

Juan Li,[*,a,b] Liuting Mo,[b] Chun-Hua Lu,[a] Ting Fu,[b,c] Huang-Hao Yang[*,a] and Weihong Tan[*,b,c]

[a] The Key Lab of Analysis and Detection Technology for Food Safety of the MOE and Fujian Province, State Key Laboratory of Photocatalysis on Energy and Environment, College of Chemistry, Fuzhou University, Fuzhou 350002, China. E-mail: lijuan@fzu.edu.cn, hhyang@fzu.edu.cn.

[b] Molecular Sciences and Biomedicine Laboratory, State Key Laboratory for Chemo/Biosensing and Chemometrics, College of Chemistry and Chemical Engineering and College of Biology, Collaborative Innovation Center for Molecular Engineering and Theranostics, Hunan University, Changsha 410082, China. E-mail: tan@chem.ufl.edu.

[c] Department of Chemistry and Department of Physiology and Functional Genomics, Center for Research at the Bio/Nano Interface, UF Health Cancer Center, University of Florida, Gainesville, FL 32611-7200, USA Fax: (+1) 352-846-2410

Abstract

Hydrogels are crosslinked hydrophilic polymers that can absorb a large amount of water. By their hydrophilic, biocompatible and highly tunable nature, hydrogels can be tailored for applications in bioanalysis and biomedicine. Of particular interest are DNA-based hydrogels owing to the unique features of nucleic acids. Since the discovery of DNA double helical structure, interest in DNA has expanded beyond its genetic role to applications in nanotechnology and materials science. In particular, DNA-based hydrogels present such remarkable features as stability, flexibility, precise programmability, stimuli-responsive DNA conformations, facile synthesis and modification. Moreover, functional nucleic acids (FNAs) have allowed the construction of hydrogels based on aptamers, DNAzymes, i-motif nanostructures,

siRNAs and CpG oligodeoxynucleotides to provide additional molecular recognition, catalytic activities and therapeutic potential, making them key players in biological analysis and biomedical applications. To date, a variety of applications have been demonstrated with FNA-based hydrogels, including biosensing, environmental analysis, controlled drug release, cell adhesion and targeted cancer therapy. In this review, we focus on advances in the development of FNA-based hydrogels, which have fully incorporated both the unique features of FNAs and DNA-based hydrogels. We first introduce different strategies for constructing DNA-based hydrogels. Subsequently, various types of FNAs and the most recent developments of FNA-based hydrogels for bioanalytical and biomedical applications are described with some selected examples. Finally, the review provides an insight into the remaining challenges and future perspectives of FNA-based hydrogels.

Keywords: Hydrogels, Functional nucleic acids, Aptamers, Biosensors, Controlled release, Cancer therapy

1. Introduction

Containing over 90% of water, hydrogels are highly water swellable polymer networks. It is because of this significant water content that hydrogels possess a degree of flexibility similar to that of natural tissue.[1] A number of unique features, such as high biocompatibility, high flexibility and highly tunable nature, make hydrogels extremely promising in bioanalytical detection,[2] drug delivery,[3] cancer therapy,[4] and tissue engineering.[5] In particular, stimuli-responsive, or intelligent, hydrogels, which can sense surrounding environmental changes and respond accordingly, have attracted increasing attention.[6] These kinds of hydrogels can sensitively respond to a variety of physical and chemical changes, such as pH,[7-10] ionic strength[11-13] electrical field strength,[14-16] heat,[17-19] ultrasound irradiation,[20, 21] and magnetic stimuli.[22, 23] However, hydrogels that only rely on polymer properties have, as a consequence, only limited applications in the bioanalytical and biomedical fields.[24] Furthermore, the types of materials used in constructing hydrogels are still limited. These limitations have prompted scientists to develop more flexible and biocompatible hydrogels.[25] Tremendous efforts are underway to incorporate biofunctional motifs into hydrogels, including DNA,[26-28] antibodies,[29-31] polypeptides,[32, 33] and enzymes,[34-36] which has expanded the available stimuli, thereby meeting the stringent requirements for bioanalytical and biomedical applications.[37]

Of particular interest are DNA-based hydrogels for the unique features brought by nucleic acids. DNA has existed in nature for billions of years, and after the discovery of DNA double helical structure by Watson and Crick, the applications of DNA have expanded to nanotechnology and materials science.[38-40] Incorporation of DNA to construct DNA-based hydrogels presents several remarkable features. **(*i*) Stability.** Compared to antibodies and protein enzymes, DNA possesses enhanced stability

under intensive heating, pressure, and chemical processing.[41] **(*ii*) Flexibility.** The flexibility of DNA hybridization provides a rich library of building blocks for hydrogels. **(*iii*) Precise programmability.** The programmability of DNA strands, which is based on purine and pyrimidine base pairing rules and DNA secondary structures, leads to precisely predicted DNA structure. Under certain conditions, self-assembled DNA hydrogels can be achieved through sequence design, and DNA can also be incorporated into synthetic polymers to form DNA-hybrid hydrogels. **(*iv*) Stimuli-responsive DNA conformational changes leading to switchable properties.** Some functional DNAs undergo abrupt conformational changes upon external stimulation, bringing reversible and switchable changes to DNA-based hydrogels. For example, a pH-sensitive cytosine(C)-rich DNA sequence can undergo conformational changes between a four-stranded i-motif structure (pH = 5) and a random single-stranded structure (pH = 8).[42] **(*v*) Facile synthesis and modification.** DNA can be synthesized in large quantities by an automated solid-phase technique and can also be modified with many functional groups, such as acrydite, amino, carboxyl and thiol, which can react with other functional moieties. With the development of phosphoramidite chemistry, most DNA modifications can be incorporated by programming a DNA synthesizer for easy preparation and accessibility. The technique of nucleic base modification can introduce multiple functionalities into hydrogels.[43]

In spite of their potential usefulness, the idea of DNA-functionalized hydrogels is still a relatively new field, with the first publication having appeared in 1996,[44] and most developments have occurred in just the past ten years.[45-48] One specific class of DNA-based hydrogel is a functional nucleic acid (FNA)-based hydrogel. Traditionally, DNA is utilized as carrier for genetic information. However, functional nucleic acids (FNAs), such as aptamers, DNAzymes, i-motif structures, antisense DNAs, siRNAs

and CpG oligodeoxynucleotides, provide additional molecular recognition, catalytic activities and therapeutic potential, making them key players in biological analysis and biomedical applications. To date, a variety of applications have been demonstrated with FNA-based hydrogels, including biosensing,[49] environmental analysis,[50] controlled drug release,[51] cell adhesion[52] and cancer therapy.[53]

In this review, we focus on advances in the development of FNA-based hydrogels, which have fully integrated the unique features of FNAs and DNA-based hydrogels. We first introduce the different strategies for constructing DNA-based hydrogels. Subsequently, various types of FNAs and the most recent developments of FNA-based hydrogels for bioanalytical and biomedical applications are described using selected examples. Finally, the review provides an insight into the remaining challenges and future perspectives of FNA-based hydrogels.

2. Different strategies for developing nucleic acid-based hydrogels

Three general strategies were implemented to develop DNA-based hydrogels. The first strategy involves modification of hydrophilic polymer chains with DNA as chain branches and subsequent formation of DNA hydrogels by crosslinking the branches, termed DNA-hybrid hydrogels. The second strategy involves crosslinking of DNA itself to form hydrogels by enzyme ligation, polymerization, hybridization, and specific binding of DNA motifs, termed pure DNA hydrogels. The third strategy involves physical interactions, such as entanglement of DNA or electrostatic interaction between DNA and positively charged polymers to entrap DNA within polymer networks for gene therapy. In this review, we focus on the first two strategies. Further information on all three strategies can be found in several excellent reviews and references highlighted therein.[54-56]

2.1 DNA-hybrid hydrogels

Owning to the unique features of DNA, special consideration has been given to the incorporation of DNA into synthetic polymers to form DNA-hybrid hydrogels, which by the facile molecular engineering of their components, demonstrates such advantages as diversified controllability and multifunctional properties.

In 1996, Nagahara and Matsuda first reported the DNA-polymer hybrid hydrogel.[44] Two kinds of acrydite-modified ssDNAs were separately copolymerized with acrylamide monomers, thus incorporating them into polyacrylamide (PAA) chains (DNA-PAA). Then, two types of hydrogels were prepared: (*i*) a hydrogel formed by hybridization between an (oligoT)-derivatized copolymer and an oligoA as a crosslinker (Type I in Fig. l) and (*ii*) a hydrogel formed by hybridization between oligoA and oligoT attached to the side chains of corresponding copolymers (Type II in Fig. 1). These DNA-polymer hybrid hydrogels are biocompatible, and they maintain the specific recognition ability of DNA. Since then, using a similar strategy, DNA-PAA copolymers have been used to build various functional hydrogels, which have attracted attention in many fields, especially in stimuli-responsive systems.[57]

Instead of using polyacrylamide, some stimuli-responsive polymers can also be employed to construct DNA-polymer hybrid networks to expand the scope of their applications. Temperature-responsive polymer is a major class of stimuli-switchable polymers undergoing reversible temperature-controlled sol-gel phase transitions.[58-60] The most studied thermosensitive polymer is known as poly(*N*-isopropylacrylamide) (pNIPAM) and shows a low critical solution temperature (LCST) around 32 °C in aqueous solutions, which is a useful temperature for biomedical applications since it is close to body temperature (37 °C).[61] The pNIPAM hydrogels show temperature-dependent volume changes. At low temperature, water-polymer

interaction is strong, and the hydrogel is highly swollen. At temperatures higher than the LCST, hydrogen bonds between polymer and water start to break down, and the hydrogel collapses to interact with itself through hydrophobic interactions.[62] Willner and coworkers reported a bifunctional stimuli-triggered pNIPAM/DNA hydrogel by incorporation of pNIPAM into the system with additional thermosensitive property.[63] Besides thermosensitive polymers, photoresponsive DNA-hybrid hydrogels were developed by incorporating photosensitive azobenzene groups into DNA strands as crosslinkers.[64] Upon UV-vis light irradiation, *cis-trans* isomerization of azobenzene resulted in hybridization between azobenzene-incorporated DNA and its complementary strand (cDNA), which then triggered a sol-gel conversion. These hydrogels are easy to synthesize, and they can be prepared with controllable sizes and structures.

In order to create more stable DNA structures and networks capable of withstanding elevated temperatures, DNA can be chemically modified to improve its thermal stability. For example, DNA-organic molecule hybrids have been utilized for the construction of DNA structures and networks.[65-67] Psoralen, a natural product that intercalates and crosslinks DNA, is widely used to create DNA structures with enhanced thermal stability.[68] Luo and coworkers reported thermostable branched DNA hydrogels combining psoralen crosslinking and branched DNA building blocks.[69] To accomplish this, branched DNA junctions were prepared by a double-stranded core region and single-stranded primer regions (Fig. 2A). After psoralen treatment, the double-stranded core regions were chemically stabilized, while the single-stranded primer region functioned as substrate for DNA processing enzymes, such as Taq DNA polymerase, which is commonly used in polymerase chain reaction (PCR). During the PCR process, these primers were extended to form connections

among the Y-shaped DNA branches, forming a networked structure where the Y-shaped DNA branches acted as crosslinkers (Fig. 2B). After concentration of the PCR products, this network formed a DNA hydrogel, allowing for novel biotechnological applications, such as a genetically encoded gel for protein production. Remarkably, the use of PCR makes it possible to amplify DNA from low concentrations, while, at the same time, introducing functional DNAs into a hydrogel network.

This field could be further expanded by the introduction of many components to afford DNA hydrogel with more functionality and versatility. For example, Xu *et al.* prepared a DNA-graphene hybrid hydrogel based on the interaction between graphene oxide (GO) sheets and DNA in an aqueous environment.[70] The solution of double-stranded DNA (dsDNA) was mixed with aqueous GO dispersion followed by heat treatment. The dsDNA was unwound to single-stranded DNA (ssDNA) during the heating process and formed ssDNA chains bridged to adjacent GO sheets *in situ via* strong noncovalent interactions, such as π-π stacking interaction. It should be noted that simply mixing GO dispersion with ssDNA solution only produced heterogeneous hydrogels, mainly owing to the fast binding of ssDNA to GO sheets, which resulted in locally gelated particles. These hydrogels possess high mechanical strength, excellent environmental stability, high dye-adsorption capacity, and self-healing function. Similarly, in 2011, Cheng *et al.* constructed a pH-responsive DNA/single-walled carbon nanotube (SWNT) hybrid hydrogel, consisting of a linear unit (DNA duplex with a sticky domain at each end) and a crosslinking unit (SWNT wrapped by specially designed DNA structures).[71] In this case, reversible gelation behavior could be realized by altering the pH. The two components have no specific interactions when pH is higher than 6.3, thus the whole system is in solution state.

While the pH is lower than 6.3, two sticky domains could form an intermolecular i-motif structure, thus causing gelation. Remarkably, the mechanical property of the hydrogel could be adjusted by varying the concentration of hydrogel contents.

More recently, another interesting work reporting on a DNA/tannic acid hybrid hydrogel was published by Lee and coworkers.[72] Tannic acid (TA), one of the most well-known plant-derived polyphenols,[73] was found to combine with DNA to form a hydrogel, termed TNA hydrogel (TA+DNA). TA is a kind of "molecular glue" that can reversibly connect with phosphodiester bonds. These TNA hydrogels exhibited biodegradability, extensibility, tissue adhesiveness and hemostatic ability. Notably, this new DNA hydrogel was prepared without chemically modifying DNA or crosslinking by complementary sequences, thus representing a new approach for fabricating DNA-hybrid hydrogels.

2.2 Pure DNA hydrogels

The multiple steps required for modification of DNA-polymer hybrids have, to some extent, limited their progress. Recently, DNA was reported to form a hydrogel by itself under certain conditions. DNA is a remarkable polymer that can be manipulated by a large number of molecular tools including enzymes. In 2006, Luo and coworkers first reported the construction of a hydrogel entirely made from branched DNA via an enzymatic reaction.[74] In this process, DNA served as both linker and substrate. To form the DNA hydrogel, branched DNA motifs, such as X-, T-, or Y-shaped DNA (termed as X-DNA, Y-DNA, and T-DNA), were first prepared through the self-assembly of rationally designed ssDNA stands (Fig. 3A). These branched DNA stands possess self-complementary sticky ends. Through hybridization of the sticky ends, these branched motifs were first connected to form a 3D network. Then, a ligation enzyme (T4 DNA ligase) was employed to seal the nicks in the DNA

network, resulting in a stable DNA hydrogel. These DNA hydrogels were biocompatible, biodegradable, and easily molded into desired shapes and sizes. They could be loaded with drugs, proteins and even living cells, which could be released over time upon degradation of the DNA. Subsequently, the same group also successfully incorporated a functional plasmid into the hydrogel and invented a cell-free protein-producing hydrogel system.[75]

A second example of enzyme-catalyzed assembly of DNA hydrogels is a fascinating DNA hydrogel made of 3D-entangled DNA products through a combination of rolling circle amplification (RCA) and multi-primed chain amplification (MCA) processes.[76] After running RCA and subsequent MCA, a continuous chain reaction was established, thereby creating extremely long DNA molecules which resulted in a physically linked DNA hydrogel (Fig. 3B). Interestingly, these novel hydrogels possessed unique microscale internal structure and unexpected mechanical meta-properties. They behave in a manner that is either liquid- or solid-like, depending on the physical environment. They have liquid-like properties when taken out of water and solid-like properties when in water. The liquid form of the hydrogel can adapt to different shapes of the container. However, it can always rapidly return to its original shape when replaced in water. Such unique meta-properties of the DNA hydrogel may find applications in drug release, cell therapy, electric switches and flexible circuits. Moreover, by using DNA as programmable, sequence-specific “glues”, shape-controlled hydrogel units can be assembled into prescribed structures. Qi *et al.* have demonstrated that RCA reaction could generate long DNA glues to assemble PEG hydrogels, resulting in micro- and macro-scale complex structures in a programmable manner.[77] They designed complementary sequences in the RCA products so that different hydrogels could be

assembled through sequence-specific hybridization. Mixing the hydrogels in a tube under rotation produced multi-hydrogel objects with edge lengths ranging from 30 micrometers to a millimeter.

Instead of using enzymes to assist the assembly of DNA hydrogels, pure hydrogels can also form by crosslinking DNA building blocks through formation of intermolecular i-motif structures (Fig. 3C).[78] C-rich nucleic-acid strands self-assembled at pH 5.0 into an i-motif structure, which dissociated at pH 8.0 into a random coil conformation.[42] Y-shaped DNA building blocks were prepared containing cytosine-rich overhangs at each terminus. At neutral pH, no interaction existed within the assembled Y-shaped DNA structure because of electrostatic repulsion. By decreasing the pH to 5, however, these C-rich ends self-assembled to form an i-motif structure, as a result of protonation of the cytosines, in turn resulting in hydrogel formation. Addition of base to the system resulted in an immediate gel-to-sol transition, which occurred within 1 minute. Gold nanoparticles (AuNPs), as model indicators, could be trapped and released from the hydrogels following pH changes, demonstrating their potential application in biosensing and drug delivery. The use of i-motif structure as a crosslinker resulted in the stability of these hydrogels, but only at acidic pH, thus preventing their application in physiological conditions.

To address this problem, DNA hydrogels were prepared by crosslinking the DNA building blocks by sequence-directed hybridization. It has been well documented that DNA can be precisely designed with specific sequences and self-assemble into two- or three-dimensional nanostructures,[79-82] which can then be used as a programmable template to direct the assembly of nanoparticles[83-86] or fabrication of nanomotors, nanomachines and nanodevices.[87-90] Xing *et al*. recently designed two kinds of building blocks, a Y-scaffold and a linker DNA (Fig. 3D).[91] The Y-scaffold contains

three sticky ends, which are complementary with the two sticky ends of the linker DNA (dsDNA). Simply mixing the two building blocks at a proper ratio was sufficient to induce the assembly of a Y-scaffold and linker DNA by hybridization of the sticky ends. Accumulating this hybridization will lead to hydrogel formation. Changing the length and composition of sticky ends produces hydrogels with different thermostability. Moreover, they also designed a restriction enzyme sequence domain in the linker DNA structure, bringing specific enzymatic responsiveness of the hydrogels. This research further widened the application conditions of DNA hydrogels.

3. Functional nucleic acid-based hydrogels and their bioanalytical and biomedical applications

Nucleic acids are fundamental biomacromolecules that function to preserve, transfer, and express genetic information. However, in the 1980s, Cech *et al*. and Altman *et al*. discovered RNA enzymes (ribozymes) that catalyze RNA self-cleavage or RNA transesterification in splicing.[92, 93] These findings have opened doors for new research in nucleic acid chemistry and biology. Nucleic acids that can perform active roles in binding, catalysis and therapy have been termed as "functional nucleic acids" (FNAs).[94-96] These FNAs achieve their tertiary folding and activity through a combination of different molecular interactions and motifs, such as hydrogen bonds, hydrophobic interactions, van der Waals forces, canonical/non-canonical base pairs, G-quadruplexes and metal ion coordination.[97, 98] Some exciting new developments in the use of FNAs to fabricate hydrogels have appeared during the past several years in the areas of bioanalysis and biomedicine. The following section discusses various kinds of FNA-based hydrogels, as well as their applications, especially in the

bioanalytical and biomedical fields.

3.1 Aptamer-based hydrogels and their applications

Aptamers are single-stranded nucleic acids isolated from random-sequence DNA or RNA libraries by an *in vitro* selection process termed systematic evolution of ligands by exponential enrichment (SELEX).[99-101] Based on their unique secondary and tertiary structures, aptamers possess high recognition ability towards specific molecular targets that range from small inorganic and organic substances to proteins or cells.[99-107] The dissociation constants (K_d) of aptamers range from nanomolar to picomolar scale, which is comparable to the K_d of antibodies.[108] Therefore, they are often regarded as chemical antibodies. Compared with antibodies, aptamers have many advantages, such as simple synthesis, good stability and design flexibility, making them suitable candidates for DNA hydrogel engineering. Owing to their low K_d values, aptamers can specifically recognize their substrates, even at very low concentrations, and undergo structural changes upon binding or dissociation of substrates. These structural changes can stimulate specific physical or chemical interactions within hydrogel systems or circumambient solution systems. In addition, aptamers can be easily conjugated with fluorescent dyes,[109] electrochemical indicators[110] and nanoparticles,[111] thus expanding their applications. Since their first discovery in the 1990s, aptamers have become a focus in bioanalytical, diagnostic and therapeutic applications.[112-116] Furthermore, the availability of a wider range of aptamers will make aptamer-based hydrogels even more versatile in the future. Motivated by the special features of aptamers, aptamer-based hydrogels have been developed for biosensing, controlled release, cell adhesion and targeted therapy.

3.1.1 Aptamer-based hydrogels for biosensing

By their high target specificity, easy synthesis, low cost, and chemical stability, aptamers have been regarded as promising recognition tools with which to design

various sensing systems. Incorporation of aptamers into hydrogels significantly expands the range of stimuli compared with conventional hydrogels. Aptamers that recognize biomolecules can be pretrapped inside hydrogels to further diversify the available stimuli. The design is based on the competitive binding of targets to the trapped DNA aptamers.

The first aptamer-based hydrogel was designed to detect adenosine.[117] As shown in Fig. 4A, two acrydite-modified DNAs, **S-1** and **S-2**, were copolymerized with acrylamide, allowing incorporation into polyacrylamide chains **P-1** and **P-2**, respectively. When **P-1** and **P-2** were mixed, a fluid state was obtained. Then, the hydrogel was crosslinked by the hybridization of **P-1** and **P-2** with a rationally designed DNA linker strand **S-3**, which contained three functional domains: domain I (in pink) complementary with **S-1**, domain II (in green) complementary with the last five nucleotides of **S-2**, and domain III (in purple), an aptamer sequence having seven nucleotides complementary with **S-2**. In the presence of target adenosine molecules, aptamers competitively bound to targets, but the last five nucleotides of **S-2** could not remain hybridized, leading to the breakdown of the crosslinks and the disassembly of the hydrogel within 15min. This disassembly could be exploited to achieve target-responsive payload release. By their optical properties and chemical stability, AuNPs, as visual indicators, were mixed with **P-1** and **P-2** before gelation. After adding **S-3**, the formed hydrogel was immersed in a buffer solution. In the presence of adenosine, the upper buffer solution turned from colorless to red, indicating that the AuNPs had been released into the solution (Fig. 4B). This result was further confirmed by an absorption test (Fig. 4C). To further illustrate the versatility of this method, human thrombin aptamer was used to construct the hydrogel. Similar phase transition results were observed in the presence of thrombin. Owing to the larger size

of thrombin, it should be noted that its rate of diffusion into hydrogel was slow and that thrombin-induced gel-to-sol transition was much slower (130 min for 90% release) than that of adenosine. Therefore, the application of this method can be further extended by the introduction of different aptamers, and various analytes can be monitored using these platforms.[118-120]

Although using AuNPs as indicators in the above method, the sensitivity of this method was still too low for analysis. To solve this problem, Zhu *et al.*[121] used an enzyme as a tool for signal amplification. They designed an aptamer-based hydrogel to realize a sensitive visual detection of cocaine. Instead of AuNPs, amylose was chosen as a visual indicator because of its color change from yellow to dark blue in the presence of iodine. In the presence of amylase, amylose would be hydrolyzed to glucose, with no color change in the iodine-glucose solution. Based on these characteristics, amylase was trapped in the DNA-grafted polyacrylamide hydrogel. Because both amylase and amylose are large polymers, they were physically separated by the hydrogel. Thus, amylose with iodine yielded a dark blue color in the buffer solution outside the hydrogel. The crosslinker DNA was a cocaine-binding aptamer that could be competitively removed from the hydrogel by cocaine. Therefore, in the presence of cocaine, the hydrogel disassembled and released amylase to the buffer solution. Amylose was then digested by amylase, and the dark blue color disappeared. Importantly, it was not necessary for the entire gel to completely dissolve, as long as sufficient amylase was released to the solution, causing the color to weaken. Results demonstrated that this platform could detect less than 20 ng cocaine in 10 min with the naked eye.

Moreover, in order to perform a quantitative analysis, the same group introduced a glucose meter to the hydrogel detection system.[122] The authors reported a

target-responsive "sweet" aptamer-based hydrogel combined with a portable personal glucose meter (PGM) for quantitative detection of nonglucose targets. As shown in Fig. 5, strands **S-4** and **S-5** were complementary to adjacent areas of strand **S-6** containing cocaine aptamer sequence. After adding strand **S-6** to form the hydrogel, glucoamylase was trapped inside the hydrogel and physically separated from its substrate, amylose, which was in the solution outside the hydrogel. In the presence of target cocaine, strand **S-6** specifically bound with targets to form target-aptamer complexes, leading to breakdown of the hydrogel and release of glucoamylase, which catalyzed the hydrolysis of amylose to produce a large amount of glucose for quantitative readout by the PGM. The method enabled selective analysis of cocaine with a detection limit corresponding to 3.8 μM in buffer solution, 4.4 μM in urine and 7.7 μM in 50 % human plasma, indicating the applicability of this method in samples of complex body fluids. These results were consistent with those from the standard liquid chromatography/mass spectrometry (LC/MS) method, suggesting good accuracy and reliability. Since different aptamers can be used for construction, it is possible to extend this simple, portable, inexpensive and quantitative hydrogel detection method to a range of nonglucose targets.

More recently, the same group designed another quantitative analysis method for point-of-care testing (POCT) based on Au core/Pt shell nanoparticles (Au@Pt NPs)-encapsulated target-responsive hydrogel and multiplexed volumetric bar-chart chip (V-chip).[123] Au@Pt NPs can catalyze the decomposition of H_2O_2 to generate O_2, which was used for signal transduction and amplification, and a V-chip was used for visual quantitative readout. As shown in Fig. 6, the preparation of Au@Pt NPs-encapsulated target-responsive hydrogel was similar to that of the glucoamylase-trapped hydrogel mentioned above, except that Au@Pt NPs were preloaded inside the

hydrogel during its formation. The prepared hydrogel was kept in the hydrogel reservoir of the V-chip (Fig. 6A). The aptamer-target complexes formed after target cocaine was added to the reservoir, leading to dissociation of the hydrogel and release of the encapsulated Au@Pt NPs into the supernatant solution (Fig. 6E). By sliding up the V-chip, three connected horizontal channels were formed (Fig. 6C). Under negative pressure, the supernatant containing the released Au@Pt NPs was drawn into the first channel (green). H_2O_2 and the indicator red ink were injected into the second channel (yellow) and the third channel (red), respectively. By further sliding up the V-chip, the supernatant, H_2O_2 and red ink were loaded in six independent parallel connected vertical channels (Fig. 6D). Contact between Au@Pt NPs and H_2O_2 led to the catalytic decomposition of H_2O_2 to generate O_2, which pushed the red ink into the top thinner channel (Fig. 6D, F). The moving distance in each ink bar within a specified time was independently correlated with the concentration of the Au@Pt NPs catalyst, which, in turn, was proportional to target concentration. The V-chip method can detect cocaine lower than 1 μM and is also applicable to the detection of other targets by simply changing aptamer sequences. Owing to high sensitivity, selectivity, portability, and quantitative visual detection, the V-chip method has potential applications in POCT, environmental safety and food quality assurance.

Dual response was also possible by crosslinking the hydrogel with two types of aptamers, allowing for the design of logic gate systems. Aptamer-based logic gates that respond to multiple targets, or one target and some environmental stimulus, such as pH, have been described by several groups.[124-126] Tan and coworkers exploited the combination of aptamers and hydrogels to create two colorimetric logic gates (“AND” and “OR”) using cocaine and ATP aptamers as crosslinkers to form an aptamer-based hydrogel.[127] As a model, Fig. 7 shows the “AND” logic gate. In order to visualize the

gel-sol transition, the authors pretrapped AuNPs into the hydrogel as indicators. In order to achieve an "AND" gate, the hydrogel would disassemble, but only in the presence of both targets. DNA sequences were designed to form a Y-shaped structure through self-assembly of three single-stranded DNAs (strands **S-7**, **S-8** and **S-9**) (Fig. 7A). In the case of one input (ATP or cocaine), two of the three hybridizations was interrupted, but the three strands remained linked, and the hydrogel stayed intact (Fig. 7B, C). When both cocaine and ATP were introduced as inputs, the hydrogel underwent a gel-sol transition, and the entrapped AuNPs were then released to buffer solution (Fig. 7D). As a result, the buffer solution turned from colorless to red, which could be easily detected with the naked eye. For the "OR" gate, the crosslinker hybridized with both DNA strands modified on one polymer, while no interaction between the two strands took place. As such, either of the inputs could decompose the hydrogel and release the AuNPs.

Other than small organic molecules, aptamers able to recognize proteins are also implemented in hydrogels for detection of protein or virus.[128-131] Recently, Spivak and coworkers reported a bioimprinting superaptamer hydrogel for ultrasensitive and visual detection of proteins.[132] In this system, a superaptamer complex was first prepared by mixing two different polymerizable, methacrylamide-modified thrombin-binding aptamers with thrombin to form aptamer-thrombin-aptamer imprinted complexes. These complexes were then incorporated into hydrogels via free radical polymerization in which thrombin served as a crosslinker imprinted in the hydrogel. Removal of the imprinted thrombin dissolved partial crosslinkers, resulting in a swelling response of the hydrogel with increased length. Such changes in hydrogel length were reversible by reintroducing target thrombin into the hydrogel such that shortening of the length was dependent on the amount of thrombin introduced. Similarly, using platelet-derived

growth factor-BB (PDGF-BB) aptamers bound to identical sites on PDGF-BB dimeric protein, an imprinted PDGF-BB superaptamer hydrogel was developed. Removal of proteins from the hydrogel resulted in visible length increase of hydrogel in the capillary, while reintroduction of proteins gave a shrinking response. The shrinking volume of thrombin and PDGF-BB superaptamer hydrogels could be observed by the naked eye in the range of 10^{-17} to 10^{-12} mol/L and 10^{-14} to 10^{-6} mol/L protein concentration, respectively. It is remarkable that volume changes in this type of hydrogel were visible to the naked eye down to femtomolar concentrations of proteins. Furthermore, specific recognition could even be maintained in biological matrices, such as urine and tears.

Later, for virus detection, the same group reported a "Molecularly Imprinted Polymer Gel Laser Diffraction Sensor" (MIP-GLaDiS).[133] In this study, a virus-bioimprinted hydrogel was micromolded into a diffraction grating sensor by using imprint lithography. Specifically, apple stem pitting virus (ASPV), which is a filamentous virus with a capsid comprised of MT32 proteins, was chosen as a target. The mixture of aptamer against MT32 with the virus extract was prepared as the prehydrogel solution. Additional monomers were added to the prehydrogel solution and then cast onto the elastomer grating micromolds for gelation. Thus, the virus sample was imprinted into the grating-patterned hydrogel. Removal or rebinding of the virus caused the expansion or contraction of hydrogel, and the hydrogel's change of volume was then detected by passing a laser light through the hydrogel and measuring the 1D diffraction patterns with a ruler that could be read by the naked eye. The detection limit reached 10 ng/mL, with good reproducibility and selectivity against related viruses. In another example, aptamer-based hydrogels were immobilized on quartz crystal microbalance (QCM) for rapid, sensitive and specific detection of influenza virus H5N1.[134] Compared to the anti-H5 antibody-coated QCM immunosensor, the QCM sensor coated with aptamer

hydrogel demonstrated enhanced sensitivity of virus detection, with a detection limit of 0.0128 HA unit, and faster detection time within 30 min.

3.1.2 Aptamer-based hydrogels for target capture and release

Hydrogels are one of the most appealing polymeric materials for preparing capture-and-release systems for target molecules. Such systems impact drug development and regenerative medicine.[135-137] Compared with traditional hydrogels, aptamer-based hydrogels can be applied to the separation of various targets, ranging from small molecules to biomolecules, and even whole cells.

The capture and controlled release of target molecules are critical steps in designing a hydrogel system for drug delivery. Because most hydrogels have high water-absorbing abilities, targets (drugs, in most cases) can be easily released in a short time without modification. Therefore, to slow the release process and prolong drug action, different strategies have been adopted, either by modulating the interaction between the target and hydrogel matrix or by modifying the hydrogel network.[138-140] Taking advantage of interactions between aptamers and targets, Wang and coworkers reported a hydrogel functionalized with aptamers to develop a sustained release system.[141] In this study, PDGF-BB aptamer, as the affinity site, was attached to polyacrylamide gel for sustained release of PDGF-BB. Specifically, acrydite-modified aptamer and PDGF-BB were first mixed to form an aptamer/PDGF-BB complex and then transferred to a solution containing acrylamide, bis-acrylamide, ammonium persulfate (APS) and *N,N,N′,N′*-tetramethylethylenediamine (TEMED) for free radical polymerization. In order to test the sustained release of protein, the hydrogel was immersed in a release medium. Compared to native hydrogel physically mixed with PDGF-BB, the release from the aptamer-based hydrogel decreased from 70% to 10% in the first 24 h, and cumulative release reduced from 90% to 16% in 6 days. These results suggested that the

aptamer-functionalized hydrogel was successful in sustained protein release through the specific binding between aptamer and its target.

Nevertheless, it remains necessary to develop a controlled release system allowing for the triggered release at a defined time point. To accomplish this, the strand displacement technique has been used to manipulate hydrogel structural changes.[142-148] Here, complementary DNA sequences of aptamers can be used as triggers for controlled release through competitive binding of aptamer and displacement of payloads. Using this strategy, Mi and coworkers constructed a reversible hydrogel for capture and release of protein.[142] Two kinds of DNAs were grafted on polyacrylamide chains, which were designed to be partially complementary to the linker strand containing thrombin aptamer sequences. The capture of thrombin was achieved by the strong interaction between aptamer and thrombin. The hydrogel was formed by mixing the DNA-functionalized polyacrylamide with thrombin-bound linker strands. Therefore, thrombin was loaded and retained in hydrogel through aptamer binding. More than 90% of the captured thrombin was maintained in the hydrogel after soaking in buffer for a week. The crosslinking of hydrogel was found to be reversible when a fully complementary sequence of linker strand was added to the system, leading to gel dissolution and thrombin release. Later, the same group developed an aptamer-based hydrogel to separate a specific target from a mixed system.[143] Since a variety of aptamers can be incorporated into this hydrogel, this system provides a promising and convenient tool for protein release.

Indeed, the capture of biomolecules from real samples still remains challenging, given the complexity of virtual environments. Thus, effective capture of biomolecules from fluid mixtures is vital for applications ranging from target characterization in biochemistry to environmental analysis and biomedical diagnostics. Shastri *et al*.[149] recently developed a hybrid microfluidic system for biomolecule extraction from

complex solutions. This system is composed of four cooperative components: (1) compartments providing two chemically distinct environments *via* a microfluidic system; (2) a stimuli-responsive aptamer acting as an affinity handle; (3) polymeric microscopic fins attached to aptamers acting as dynamic arms moving targets between two environments; and (4) stimuli-responsive hydrogel acting as an artificial muscle to actuate the arms' movement. In this system, the selected aptamer and hydrogel were both pH-sensitive. The aptamer specifically bound to thrombin at pH range 6-7, but was reversibly denatured and lost affinity for thrombin at low pH (Fig. 8A). Similarly, a pH-sensitive and biocompatible poly(acrylamide-co-acrylic acid) hydrogel was chosen as the dynamic arm able to undergo significant volumetric changes at pH 4.25 (Fig. 8B). The synchronization of reversible aptamer-thrombin binding and hydrogel volume changes provided the coordinated transport of thrombin between two environments for effective extraction of biomolecules. As shown in Fig. 8C, when fluid mixture was flowed into the top layer at pH 6.3, which corresponds to the highest binding efficiency of the aptamer, target molecules were selectively captured. When the pH value of the bottom layer shifted between 3.2 and 7.2, in acidic condition, hydrogel shrinkage would induce bending of the microscopic fins, subsequently leading to target release from denatured aptamers. In basic condition, the system returned to initial states, ready for another round of target capture. The reversibility of hydrogel volume change and aptamer folding allowed for continuous separation of targets for multiple rounds, ensuring the sufficient capture and detection of target molecules. Indeed, the recovery test showed that nearly 95.5% of the total ingoing thrombin was captured after eight rounds of recycling. Further data demonstrated the selectivity of this system. The target protein thrombin could be selectively captured from a mixture of thrombin and transferrin, thrombin and BSA, or human serum containing thrombin, leaving the

interfering protein in the top layer of fluid. These results showed high performance on concerted capture-and-release of target molecules from a fluid mixture by this chemo-mechanical sorting system.

3.1.3 Aptamer-based hydrogels for cell adhesion

Regulating cell-material surface interaction is significant for a variety of biological and biomedical applications, such as biological separation, tissue repair and wound healing. The high-affinity and -specificity interactions between aptamers and receptors on the cell surface provide an effective means of cell adhesion. Aptamer-functionalized hydrogels were constructed for dynamic control of cell adhesion.

In order to regulate cell behavior, Chen *et al.* immobilized aptamers on PEG hydrogel to provide cell binding sites, which effectively induced cell-type specific adhesion to the hydrogel without affecting cell viability.[150] The target cell density increased to 850 cells/mm^2 after aptamer incorporation from less than 5 cells/mm^2 for the control hydrogel. In addition, attenuated cell adhesion could be achieved by inactivation of aptamers using their complementary DNAs. Besides using strand displacement, restriction endonuclease was also employed in hydrogels for cell detachment.[151]

Recently, Li *et al.* adapted the original strand displacement strategy (Fig. 9).[152] As shown in Fig. 9B, a primary complementary sequence (primary CS, strand **S-10**) was initially tethered to the hydrogel, which hybridized with aptamer (strand **S-11**) and led to target cell capture via multivalent aptamer-receptor interactions. After aptamer hybridization, the target CCRF-CEM (T cell acute lymphoblastic leukemia cell line) cell density on hydrogel was observed to be 2519 ± 284 cells/mm^2, while only 6 ± 4 cells/mm^2 control cells were detected. Upon addition of a secondary CS (strand **S-12**), the fully complementary sequence of aptamer, a strand displacement procedure was triggered, and the conformation change of aptamer induced the release of aptamers and

target cells. It was found that more than 95% of cells were released within 10 min with over 99% viability. The whole procedure of cell capture and release took place under physiological conditions without any destructive factor. Hydrogel functionality is regenerable, suggesting its potential in numerous biological and biomedical applications. Later, cell attachment of hydrogel was further enhanced by implementing polyvalent aptamer, in which multiple aptamers were hybridized with one backbone as side units for polyvalency of target cell binding, leading to more cell binding with equal amounts of surface reaction sites.[153, 154]

More recently, Li *et al.* synthesized a new dynamic hydrogel for reversible and nondestructive cell adhesion controlled by molecular reconfiguration of an encrypted ligand.[155] As illustrated in Fig. 10A, the encrypted aptamer sequence (strand **S-13**) has two functional domains: cell binding domain containing aptamer sequence (in green) and blocking domain (in orange) partially hybridized with the cell binding domain. This intramolecular hybridization of **S-13** led to an inert state of aptamer, which inhibits cell adhesion. However, upon addition of unblocking sequence (strand **S-14**), the cell adhesion function was activated through the hybridization between **S-14** and the **S-13** blocking domain. Next, in order to realize cell detachment, a recovering sequence (strand **S-15**) was applied to neutralize and dissociate the **S-14** sequence from the blocking domain, returning **S-13** to its encrypted state and returning the hydrogel to its inert state so that it would be available for a new round of cell capture and release. Thus, the cell adhesion function of hydrogels can be modulated by using unblocking and recovering sequences (Fig. 10B). Compared to the initially inert hydrogel, treatment of **S-14** sequence increased cell adhesion by two orders of magnitude, while **S-15** treatment led to the detachment of 99% of cells from the hydrogel. Moreover, since molecular reconfiguration does not induce any loss or cleavage of ligand from the hydrogel, the

cell adhesion function can be reversibly controlled for multiple cycles by treatment of **S-14** and **S-15** sequences.

3.1.4 Aptamer-based hydrogels for targeted therapy

Current cancer therapy, including chemotherapy and radiotherapy, often lacks tumor cell specificity, putting cancer patients at risk for severe toxic effects. Recently, the active and cell-specific targeting of nanomaterials has begun to represent a potentially powerful technology in cancer treatment.[156] Active targeting is achieved by conjugating nanomaterials with targeting ligands that bind to overexpressed antigens or receptors on target cells.[157] This specific binding to target cells leads to an increased accumulation of nanomaterials on target cells, while minimizing harmful toxicity to nontarget cells. Therefore, combining the unique features of hydrogels and specific recognition ability of aptamers will allow for the design of aptamer-based hydrogels with decreased side effects and enhanced therapeutic efficacy.

The first example is near-infrared light-responsive core-shell nanohydrogels for targeted drug delivery.[158] Gold-silver nanorods (Au-Ag NRs) can absorb light energy in the near-infrared (NIR) range and generate heat to cause an increase of temperature in the surrounding area, which can then be used to manipulate heat-sensitive events, such as DNA hybridization. As shown in Fig. 11, Au-Ag NRs were used as templates for colloid-based polymerization. In one part, acrylamide monomers and acrydite-modified strand A **(S-16)** were first linked with a methacryl group on Au-Ag NRs to form a multiple linear polyacrylamide polymer conjugate. In another part, acrydite-modified strand B **(S-17)** and acrydite-modified aptamer sequence **(S-18)** were incorporated to obtain polymer chains. The crosslinker DNA strand **(S-19)**, which hybridized with strands (**S-16**) and (**S-17**), resulted in the formation of core-shell nanohydrogels. Aptamer sequence **(S-18)** was selected for the binding of

CCRF-CEM cells. Upon irradiation of NIR light, the Au-Ag NRs elevated the temperature of the surrounding nanohydrogels. When the temperature was higher than DNA melting temperature, double-stranded DNA dissociated, resulting in breakdown of the nanohydrogels. Meanwhile, the payload of anticancer drugs (Dox as a model) was released to generate therapeutic effect. After irradiation, cell viability results showed that the drug release process resulted in apoptosis in 67 ± 5 % CCRF-CEM cell deaths, while less than 10 % of control Ramos cells died. This study takes advantage of the aptamer as a recognition element and the nanohydrogels as a drug carrier, demonstrating the potential of this system for targeted cancer therapy.

The use of pure DNA molecules as building blocks for hydrogel construction has attracted substantial attention in the form of smart devices and precisely defined nanostructures at the nanometer scale for sensing, drug delivery and cancer therapy.[159-162] In a related study, Tan's group designed a self-assembled pure DNA nanohydrogel with controllable size and stimuli-responsive property for targeted cancer therapy.[163] As illustrated in Fig. 12, this DNA nanohydrogel was created through a self-assembly process using three kinds of building units, termed Y-shaped monomer A (YMA), Y-shaped monomer B (YMB), and DNA linker (LK), respectively. YMA serves as a building unit with three sticky ends. YMB has one sticky end and an aptamer moiety, which serves as both a blocking unit to inhibit the extension of nanoparticles and a targeting unit to recognize specific cancer cells. LK is a linear duplex DNA with two sticky ends. Hybridization of the sticky ends of monomers and LK leads to nanohydrogel formation. To design stimuli-responsive DNA nanohydrogels for targeted gene therapy, different functional elements, including antisense oligonucleotides capable of inhibiting cell proliferation, DNAzymes capable of inhibiting cell migration, and aptamers capable of targeting

specific cancer cells and disulfide linkages, can be incorporated into different building units. In addition, the DNA nanohydrogels were size-controllable by varying the ratio of YMA to YMB. The designed nanohydrogels were stable during blood circulation and were efficiently cleaved in the intracellular reductive environment, resulting in the dissociation of nanohydrogels and release of multiple therapeutic genes. After aptamer incorporation, the synthesized aptamer-based nanohydrogels could strongly inhibit cell proliferation and migration of target A549 cells, but not control cells, suggesting the potential for targeted gene regulation therapy.

3.2 Catalytic nucleic acid-based hydrogels and their applications

Catalytic nucleic acids (DNAzymes or ribozymes) represent sequence-specific nucleic acids mimicking the function of native enzymes. The first type of ribozymes discovered was a self-splicing RNA.[164, 165] Since then, ribozymes have been identified in a number of various biological settings, including *in vitro* experiments.[166-168] Deoxyribozymes (DNAzymes) are catalytic DNA structures obtained by *in vitro* selection.[169] The first kind of DNAzyme, which was capable of catalyzing a transesterification reaction in the presence of Pb^{2+} ions, was discovered in 1994 by Breaker and Joyce, demonstrating that ssDNA could indeed act as a catalyst similar to ribozymes and proteins.[170] After that, numerous non-natural catalytic nucleic acids were developed, including the hemin/G-quadruplex horseradish peroxidase (HRP)-mimicking DNAzyme,[171] metal ion-dependent DNAzymes, e.g., Mg^{2+},[172] Cu^{2+},[173] Hg^{2+},[174, 175] Zn^{2+},[176] Ca^{2+},[177] Pb^{2+},[178] UO_2^{2+}-dependent DNAzymes,[179] and cofactor-dependent DNAzymes, e.g., histidine-dependent DNAzyme,[180] as well as many other catalytic nucleic acids.[181-183] These nucleic acids have catalytic capability similar to that of protein enzymes and possess the advantages of thermostability, low-cost synthesis and easy modification, making DNAzymes attractive elements for biosensing and biotechnological applications,

such as biosensors for metal ions and other molecules,[184-186] components for DNA-based logic gates,[187, 188] components for nanomotors,[189, 190] and building units for nanomaterial assembly, including hydrogels.[191-196]

For example, HRP-mimicking DNAzyme is a complex of hemin-intercalated G-quadruplex, which can catalyze the H_2O_2-mediated oxidation of $ABTS^{2-}$ to the colored product $ABTS^{\bullet-}$ with the reduction of H_2O_2 to H_2O,[192] or lead to the generation of chemiluminescence in the presence of H_2O_2/luminol.[193] This class of DNAzyme has been widely used as an amplifying label for biorecognition and biosensing events. Recently, Willner's group reported a switchable catalytic DNA hydrogel.[194] Acrylamide units and guanine (G)-containing oligonucleotide-tethered acrylamide units were first copolymerized to copolymer chains. The addition of K^+ and hemin induced the formation of interchain G-quadruplex and yielded hemin/G-quadruplex-crosslinked hydrogel. Absorbance change of $ABTS^{\bullet-}$ and chemiluminescence of luminol confirmed the catalytic oxidation of $ABTS^{2-}$ by H_2O_2 to $ABTS^{\bullet-}$. Moreover, treatment of the hydrogel with 18-crown-6 ether caused the elimination of K^+ and subsequent disassociation of hydrogel. By cyclic addition of K^+ ions and 18-crown-6 ether, the hydrogel underwent reversible formation and separation, and the catalytic activity of hydrogel could be switched to "ON" or "OFF" states repeatedly.

Another type of DNAzyme, metal ion-dependent DNAzymes, has also attracted attention in the fabrication of hydrogels. In 2011, Lin *et al.* first reported the use of Cu^{2+} ion-dependent DNAzyme as a hydrogel crosslinker for the visual detection of Cu^{2+} ions.[195] In this system, DNAzyme and substrate strands were incorporated into linear polyacrylamide, respectively. Gelation was achieved by mixing the two polymers and the hybridization between two strands. AuNPs, as colorimetric indicators, were also encapsulated inside the matrix before gelation. In the presence of Cu^{2+} ions, the substrate

strands were irreversibly cleaved, leading to hydrogel disassembly and release of AuNPs for semi-quantitative visual detection. This hydrogel could selectively detect less than 10 nM of Cu^{2+} ions by the naked eye within 1.5 hours.

This method can be further extended to other metal ion sensors by using corresponding DNAzymes. For instance, the same group later developed a Pb^{2+}-responsive hydrogel using the same strategy, and Pb^{2+} ions as low as 10 nM could be detected by the naked eye.[196] Furthermore, in order to achieve quantitative visual detection, they combined DNAzyme hydrogels and V-chip as the readout apparatus for rapid, sensitive, portable and quantitative detection of Pb^{2+} ions. In this system, the indicators were replaced with Au@Pt NPs, and in the presence of Pb^{2+} ions, the release of Au@Pt NPs from hydrogel could efficiently catalyze the decomposition of H_2O_2 to produce O_2 gas, which led to the movement of ink bars in the V-chip, with the detection limit reaching 2.6 nM.

More recently, Willner and coworkers reported the programmed dissolution of three different metal ion-dependent DNAzyme hydrogels for activation of an enzyme cascade.[197] In this study, hydrogels were prepared by the crosslinking of DNA-modified acrylamide chains with DNAzymes and their substrates. Three different metal ion-dependent DNAzymes were used, including Cu^{2+}-, Mg^{2+}-, and Zn^{2+}-dependent DNAzymes. Meanwhile, three different enzymes, including β-galactosidase (β-Gal), glucose oxidase (GOx) and horseradish peroxidase (HRP), were immobilized in different DNAzyme-bridged hydrogels, respectively. In the presence of the respective ions, the substrates of the corresponding DNAzymes were cleaved, leading to the dissolution of hydrogels and the release of enzymes. By mixing different DNAzyme-bridged hydrogels, selective and programmed hydrogel dissolution and enzyme release could be achieved, thus activating bi- or trienzyme cascades.

3.3 Metallo-base pairs-based hydrogels and their applications

Natural Watson-Crick base pairs play a critical role in double helical nucleic acids which are responsible for the storage and transfer of genetic information. Although natural base pairs have been amazingly sophisticated throughout the long history of evolution, synthetic chemists have devoted considerable efforts in recent decades to create alternative base pairing systems to extend the information-encoding capabilities of nucleobases.[198-201]

Most of these new base pairings were designed by rearranging the hydrogen-bonding patterns using hydrophobic interactions or metal coordination. It is well known that metal coordination plays various roles in maintaining and stabilizing biologically important structures in terms of molecular recognition and catalytic activity. Recently, base pairing based on metal ion coordination, termed metallo-base pairs, has been developed and has gained increasing attention.[202-204] Here, hydrogen bonded Watson-Crick base pairs are replaced by metal-ligand interactions inside the DNA double helix, and a resultant metallo-base pair is formed and stabilized through coordination of the ions with the oligonucleotides. Among all metallo-base pairs, thymine-Hg(II)-thymine (T-Hg-T) base pairs are the best known. In this construct, the imino protons of thymine bases are substituted with Hg(II), and one Hg(II) crosslinks two N_3 atoms of thymines.[205-207] Similarly, a cytosine-cytosine mismatch pair can be altered to a stable, neutral metallo-base pair in the presence of Ag^+ ions (cytosine-Ag(I)-cytosine, C-Ag-C).[208, 209] Such metallo-base pairs have been successfully used in a wide range of applications, such as DNA biosensors for detection of metal ions, construction of DNA nanomachines and fabrication of logic gates.[210-212]

Conjugation of such metallo-base pairs into hydrogels has also attracted considerable attention for detection and removal of hazardous ions.[211-213] In 2010, Dave *et al*.

demonstrated a thymine-rich DNA-functionalized hydrogel for simultaneous detection and removal of mercury in water.[211] Specifically, the hydrogel was composed of a polyacrylamide matrix immobilized with sequences rich in thymine, and SYBR Green I dye was used as an indicator. In the absence of Hg^{2+} ions, tethered DNA adopted a random coils structure, and the addition of SYBR Green I produced weak yellow fluorescence. In the presence of Hg^{2+} ions, the DNA folded into a hairpin structure, which bound to SYBR Green I and generated green fluorescence. Thus, the detection of mercury could be observed by the fluorescence signals from SYBR Green I, which was induced by the interaction between Hg^{2+} ions and thymines. The fluorescence change could be easily observed with a detection limit of 10 nM in 50 mL water. Removal of Hg^{2+} ions from water was mainly dependent on polyacrylamide adsorption. The combination of high selectivity of T-Hg-T base pairs and high binding affinity of gel matrix provided high detection sensitivity and adsorption capacity. Later, the same group made further efforts to optimize this system, and detection sensitivity was enhanced by manipulating electrostatic interactions among SYBR Green I, DNA and hydrogel backbone.[212] Faster kinetics of signal generation was achieved by replacing the monolithic hydrogels with microparticles, shortening diffusion distance and reaching a stable signal faster.[213]

In another application taking advantages of T-Hg-T base pairs in the construction of hydrogel, Ye *et al*. developed colloidal photonic crystal hydrogel (CPCH) films for visual detection of heavy metal ions, such as Hg^{2+} and Pb^{2+} ions (Fig. 13).[214] The CPCHs were derived from a colloidal crystal array of monodisperse silica nanoparticles from periodic variation in the refractive index. Colloidal crystals endow CPCHs with some interesting optical properties, such as photonic band gaps (PBGs).[215-217] Therefore, a colorimetric CPCH-based sensor could be obtained by introduction of colloidal crystals

into target-responsive hydrogel. In this study, the colloidal crystals were polymerized within a polyacrylamide hydrogel, and T-rich oligonucleotides were then immobilized in the hydrogel matrix by EDC/NHS coupling. When exposed to Hg^{2+} ions, the hydrogel underwent shrinkage as a result of the conformational changes of T-rich sequences, leading to a change in the PBGs accompanied by a visually perceptible color change (Fig. 13B). The shift value could be used for quantitative analysis of the target metal ions. As shown in Fig. 13C, with the increased concentration of Hg^{2+} ions, the degree of shrinkage of CPCHs was enhanced, suggesting that more T-Hg-T complex structures were formed inside CPCHs. Depending on their shrinkage, the color and the diffraction peak of CPCHs underwent a blue shift. The shift value could be used to quantitatively estimate the amount of Hg^{2+} ions with a wide concentration range and a detection limit of 10 nM. Also, by using the same approach, Pb^{2+} ions binding DNA-based CPCHs could be used for visual detection of Pb^{2+} ions with a detection limit of 1 nM.

Besides coordination between thymine and Hg^{2+} ions, a cytosine-Ag(I)-cytosine (C-Ag-C) bridge was also implemented for hydrogel formation. Using this strategy, Willner's group reported reversible and switchable DNA hydrogels triggered by addition or elimination of Ag^{+} ions.[63, 218] In another work, a fluorescence DNA hydrogel immobilized with silver nanoclusters (Ag NCs) was reported.[219] By incorporating loops of unpaired cytosine bases into Y-shaped DNA building blocks, Ag NCs were stabilized in the loop domain in the presence of Ag^{+} ions and $NaBH_4$. Addition of duplex crosslinker induced the formation of Ag NCs-modified DNA hydrogel. The fluorescence property of the hydrogel was preserved when undergoing thermally reversible hydrogel solution transition, indicating good thermostability of this system.

3.4. i-motif structure-based hydrogels

The i-motif structure is a DNA quadruplex structure which can form in sequences rich

in cytosine. Stabilized by acidic conditions, they are comprised of two parallel-stranded DNA duplexes held together in an antiparallel orientation by intercalated, cytosine-cytosine^{+} base pairs.[42, 220] It was initially discovered by Gehring, Leroy and Guéron in 1993.[221] Since then, the i-motif structure has offered more choices in manipulating three-dimensional structures, and pH-dependent stabilization can modulate the assembly of different DNA nanostructures. Several applications in DNA nanotechnology have emerged owing to its unique properties.[222] Moreover, pH plays a key role in many biological functions in that knowledge of the pH of blood or physiological fluids is of great importance. Therefore, introduction of i-motif structure into DNA hydrogels will expand its biosensing and biomedical applications.

In 2009, Liu and coworkers reported a pH-responsive DNA hydrogel using i-motif structure as a crosslinker.[78] For more accurate operation of hydrogel systems, Willner's group reported a dual-stimuli-responsive pNIPAM/DNA hydrogel.[63] In this system, a C-rich DNA sequence-functionalized acrylamide monomer was copolymerized with pNIPAM chains. At acidic conditions (pH = 5.2), the tethered oligonucleotides could fold into i-motif structure, leading to the formation of a three-dimensional hydrogel network in solution. At basic conditions (pH = 8.0), unfolding of i-motif structures led to the disassembly of hydrogel, transferring the system to solution state. Meanwhile, as a thermosensitive polymer, pNIPAM endowed the hydrogel with temperature-controlled effects. Subjecting this system to heating/cooling cycles of 45°C and 25°C resulted in reversible gel-sol transition. Such pH-triggered thermosensitive hydrogels paved the way for the construction of sensors and drug delivery systems.

Apart from thermosensitivity, DNA hydrogels can be tailored with shape-memory properties. More recently, the same group demonstrated pH-switchable, shape-memory DNA hydrogels (Fig. 14).[223] In this study, two crosslinking elements were implanted into

PAA hydrogel. One was a C-rich sequence corresponding to i-motif structures as the stimuli-responsive element (strand **S-20**), and the other was a set of self-complementary sequences for duplex formation as the shape-memory element (strand **S-21**). In their design, C-rich strands assembled into i-motif structure at pH 5.0, and both i-motif structure and duplex acted cooperatively to form a stiff hydrogel. At pH 8.0, i-motif structure disassembled, transferring the hydrogel into quasi-liquid phase, yet the residual duplex network offered shape-memory code for hydrogel recovery. By repeatedly switching pH between 5.0 and 8.0, the material underwent reversible transition between predesigned shaped hydrogel and quasi-liquids.

3.5. Therapeutic nucleic acid-based hydrogels

Therapeutic oligonucleotides include a wide range of nucleic acids with different functional properties, such as antisense, RNA interference and immunorecognition.[224-226] The first suggestion that oligonucleotides might be used as therapeutics dates back to 1978 when antisense oligonucleotides were reported on the inhibition of virus replication.[227, 228] Afterwards, increasing pharmacological effect of oligonucleotides has been exploited. Besides antisense oligonucleotides, translation of RNA may be suppressed by short interfering RNAs (siRNAs) and microRNAs.[229-232] siRNAs are double-stranded RNA molecules capable of sequence-specific gene knockdown. First discovered by Fire *et al.* in 1998,[233] they were successfully used in 2002 for gene silencing in mice for hepatitis,[234] thus gaining attention and advancement for the treatment of various diseases, including cancer and infections.

It is easy to incorporate therapeutic oligonucleotides into DNA-based hydrogels based on their nucleic acid nature. Hong *et al.* reported a siRNA microhydrogel self-assembled through sense/antisense complementary hybridization and condensation with cationic polymer for gene silencing (Fig. 15).[235] In particular, sense/antisense green fluorescent

protein (GFP) siRNA with a thiol group reacted with trimeric crosslinker tris-2-maleimidoethyl-amide (TMEA) to prepare Y-shaped siRNAs or with a dimeric crosslinker 1,8-bis(maleimidodiethylene) glycol [$BM(PEG)_2$] for dimeric siRNAs. Different combinations of siRNA units led to the formation of different types of products. The first type is multimeric siRNAs, named M-siRNA, which results from the combination of dimeric sense/antisense siRNAs. The second one is moderately branched siRNAs, named DY-siRNA, resulting from the combination of dimeric, linear sense and Y-shaped antisense siRNAs, and the third one is highly branched siRNAs, resulting from the combination of Y-shaped sense/antisense siRNAs and termed YY-siRNA. The siRNA microhydrogels were condensed by a cationic polymer, linear polyethylenimine (LPEI), leading to the formation of compact and stable nanoparticles below 120 nm in size with enhanced stability and higher cellular uptake efficiency. The results showed that DY- and YY-siRNA hydrogels efficiently reduced GFP expression in MDA-MB-435 cells by 58.9 ± 1.1% and 50.8 ± 1.4%, respectively, suggesting that these hydrogels could enhance endocytosis efficiency and therapeutic efficacy.

In another work by Hong *et al.*, a siRNA hydrogel was prepared by crosslinking between siRNA and LPEI and modified with disulfide.[236] The resulting hydrogel contained inter- and intramolecular networks, demonstrating excellent structural stability during intracellular translocation, while prone to dissociate in cytoplasm, releasing free siRNAs for gene silencing.

Another widely applied therapeutic oligonucleotide is unmethylated cytosine-phosphate-guanine dinucleotides (CpG), a potent activator of innate and acquired immune responses. The CpG sequence is prevalent in bacterial genomes, while only occasionally seen in mammalian genomes. Therefore, it is considered to be a signal of pathogen invasion by the immune system, which is recognized by Toll-like receptor 9

(TLR9), followed by induction of immune response.[237] Since the elucidation of immunomodulation effect of CpG, various therapeutic applications have been reported in treatments for infection, allergy prevention and cancer immunotherapy.[238] Although oligonucleotides possess significant therapeutic potential, a major hurdle for their successful application remains the delivery strategy to target cells.

DNA-based hydrogels can also enhance the therapeutic efficacy of chemotherapy and immunotherapy. In 2011, Nishikawa *et al.* developed a DNA hydrogel consisting of CpG motifs and intercalated doxorubicin (Dox) as a sustained drug delivery system for tumor chemo/immunotherapy.[239] In this system, building units consisted of X-shaped DNA with CpG motifs, and the palindromic sequences at the 5' ends of DNA were ligated to form a CpG DNA hydrogel using T4 DNA ligase. Compared to its components or CpG free counterpart, CpG DNA hydrogels could induce higher levels of cytokine release from murine macrophage-like RAW264.7 cells, as well as maturation of murine dendritic DC2.4 cells. Dox was then incorporated into the hydrogel and slowly released with hydrogel degradation. Effective growth inhibition of murine adenocarcinoma colon26 tumor in mice was observed after intratumoral injection of Dox/CpG DNA hydrogels, taking advantage of elevated immune response induced by CpG motifs and cytotoxicity by Dox.

However, the administration of these bulky hydrogels required surgical incision, or breaking them down into fragments small enough for injection. Furthermore, the contaminating ligase had the potential of causing unwanted side effects, including anaphylactic shock. To address these issues, they further developed an injectable, ligase-free and immunomodulatory DNA hydrogel for antigen delivery.[240] In this study, several polypod-like DNAs (polypodna) containing CpG motifs were designed as building blocks. The single-stranded 5'-ends of polypodna were extended to hybridize

under physiological conditions. These hydrogels were easily injected using a fine gauge needle, and gelation occurred almost instantly following injection. Immunization with CpG DNA hydrogel loaded with ovalbumin (OVA) elicited strong cytotoxic T lymphocyte (CTL) response against EG7-OVA cells, showing higher potency and lower toxicity than OVA injected with clinical vaccine adjuvants. Removal of CpG motifs from the hydrogel resulted in a sharp decrease in immune response, indicating the significance of immunostimulation by CpG DNA hydrogel.

4. Conclusions and perspectives

Advances in biochemistry and materials science have sparked interest in the development of various biocompatible materials for bioanalytical and biomedical applications. Based on their high biocompatibility, high flexibility, low toxicity and highly tunable nature, hydrogels are promising materials in bioanalytical and biomedical applications. On the other hand, functional nucleic acids (FNAs), including aptamers, DNAzymes, i-motif structures, siRNAs and CpG motifs, provide additional molecular recognition, catalytic activities, and therapeutic potential, affording potential applications for diagnosis and therapeutics. Incorporation of FNAs into hydrogel systems can be manipulated with additional properties, significantly expanding the applications of DNA-based hydrogels, as demonstrated by the selected examples described in this review. Thus far, FNA-based hydrogels have been implemented to design sensors, separation platforms, cell adhesion platforms, controlled drug delivery and targeted cancer therapy methods. In addition, it should be noted that the use of FNA-based hydrogels for novel applications, such as molecular logic gates, mechanical actuators, and portable detection devices, has been achieved. Although these studies are still in the preliminary stage, they represent promising

potential uses of these hydrogels.

However, to further move the applications of FNA-based hydrogels forward, several challenges must be addressed. **First,** colorimetric visual detection methods based on hydrogel phase changes provide simple and rapid detection of various targets, but the problems of sensitivity and quantification have limited their applications. Incorporation of enzyme-catalyzed signal amplification mechanisms (e.g., amylase/iodide system), cascade reactions (e.g., trienzyme cascades based on β-Gal/GOx/HRP) and other signal amplification strategies can improve sensitivity. Furthermore, the detection of targets in real samples remains challenging, given the complexity of virtual environments. Therefore, development of simple and sensitive sensors capable of analyzing targets in complex biological samples should be a prospective direction for hydrogel-based sensors. **Second,** some FNA-based hydrogel systems lack efficient and precise release mechanisms, leading to premature release. The design of dual-responsive hydrogels can be used for precisely controlled cargo release. For example, incorporation of pNIPAM into polyacrylamide gel will give the hydrogel additional thermosensitive property. In addition, light-sensitive property can be regulated by incorporating azobenzenes, and pH-sensitive property can be achieved by i-motif structure. Other types of stimuli, such as NIR irradiation and magnetic fields, can also be explored. In dual-responsive hydrogels, hydrogel transitions can be triggered only in the presence of both stimuli, thus leading to more accurate operation of FNA-based hydrogel systems. **Third,** the bulky size of some FNA-based hydrogels curtails their biomedical applications. The development of methods for preparation of nanohydrogels and effective delivery of nanohydrogels into cells will expand the scope of *in vivo* applications.

Finally, although FNA-based hydrogel systems appear to hold promise for

controlled release and targeted cancer therapy, some issues remain to be resolved, such as poorly understood pharmacokinetics, long-term toxicity and off-target effects. To realize the full potential and overcome the challenges of such hydrogels, it is necessary to perform more stringent *in vivo* studies to further understand the behavior of these hydrogels. Furthermore, in-depth studies in animal models for the evaluation of safety and efficacy of these hydrogels will lay the foundation for further clinical applications. Future efforts should focus on improving these hydrogels for clinical use. Through collective efforts, we believe that the integration of further developments in materials science and nanotechnology will promote the development of FNA-based hydrogels for a variety of practical bioanalytical and biomedical applications.

Acknowledgements

The authors gratefully acknowledge the financial support from the National Natural Science Foundation of China (No. 21505021, 21125524, 21221003, 21327009, 21475026), the National Institutes of Health (GM079359 and CA133086), the National Key Scientific Program of China (2011CB911000) and China National Instrumentation Program 2011YQ03012412.

References:

1. P. H. Kouwer, M. Koepf, V. A. Le Sage, M. Jaspers, A. M. van Buul, Z. H. Eksteen-Akeroyd, T. Woltinge, E. Schwartz, H. J. Kitto and R. Hoogenboom, *Nature*, 2013, **493**, 651-655.
2. J. H. Holtz and S. A. Asher, *Nature*, 1997, **389**, 829-832.
3. Y. Qiu and K. Park, *Adv. Drug Delivery Rev.*, 2001, **53**, 321-339.
4. D. Seliktar, *Science*, 2012, **336**, 1124-1128.
5. S. Van Vlierberghe, P. Dubruel and E. Schacht, *Biomacromolecules*, 2011, **12**, 1387-1408.
6. Y. Osada, H. Okuzaki and H. Hori, *Nature*, 1992, **355**, 242-244.

7. A. Richter, G. Paschew, S. Klatt, J. Lienig, K.-F. Arndt and H.-J. P. Adler, *Sensors*, 2008, **8**, 561-581.

8. E. Cheng, Y. Xing, P. Chen, Y. Yang, Y. Sun, D. Zhou, L. Xu, Q. Fan and D. Liu, *Angew. Chem. Int. Ed.*, 2009, **48**, 7660-7663.

9. R. Marcombe, S. Cai, W. Hong, X. Zhao, Y. Lapusta and Z. Suo, *Soft Matter.*, 2010, **6**, 784-793.

10. S. L. Zhou, S. Matsumoto, H. D. Tian, H. Yamane, A. Ojida, S. Kiyonaka and I. Hamachi, *Chem. Eur. J.*, 2005, **11**, 1130-1136.

11. R. S. Zhang, M. G. Tang, A. Bowyer, R. Eisenthal and J. Hubble, *Biomaterials*, 2005, **26**, 4677-4683.

12. B. Zhao and J. S. Moore, *Langmuir,* 2001, **17**, 4758-4763.

13. T. Traitel, J. Kost and S. A. Lapidot, *Biotechnol. Bioeng.*, 2003, **84**, 20-28.

14. A. Guiseppi-Elie, *Biomaterials*, 2010, **31**, 2701-2716.

15. R. V. Kulkarni and B. Sa, *J. Bioact. Compat. Polym.* 2009, **24**, 368-384.

16. R. V. Kulkarni and S. A. Biswanath, *J. Appl. Biomater. Biomech.*, 2007, **5**, 125-139.

17. S. Maeda, T. Kato, H. Kogure and N. Hosoya, *Appl. Phys. Lett.*, 2015, **106**,171909.

18. I. Asmarandei, G. Fundueanu, M. Cristea, V. Harabagiu and M. Constantin, *J. Polym. Res.*, 2013, **20**, 293

19. Q. Q. Wang, M. Kong, Y. An, Y. Liu, J. J. Li, X. Zhou, C. Feng, J. Li, S. Y. Jiang, X. J. Cheng and X. G. Chen, *J. Mater. Sci.*, 2013, **48**, 5614-5623.

20. R. Ebrahimi and M. Ebrahimi, *J. Polym. Eng.*, 2014, **34**, 625-632.

21. B. Rokita, J. M. Rosiak and P. Ulanski, *Macromolecules*, 2009, **42**, 3269-3274.

22. T.-Y. Liu, S.-H. Hu, K.-H. Liu, D.-M. Liu and S.-Y. Chen, *J. Control. Release*, 2008, **126**, 228-236.

23. Y.-Y. Liang, L.-M. Zhang, W. Jiang and W. Li, *Chemphyschem*, 2007, **8**, 2367-2372.

24. N. A. Peppas, J. Z. Hilt, A. Khademhosseini and R. Langer, *Adv. Mater.* , 2006, **18**, 1345-1360.

25. W. E. Hennink and C. F. van Nostrum, *Adv. Drug Delivery Rev.*, 2002, **54**, 13-36.

26. F. Wang, X. Liu and I. Willner, *Angew. Chem. Int. Ed.*, 2015, **54**, 1098-1129.

27. X. Xiong, C. Wu, C. Zhou, G. Zhu, Z. Chen and W. Tan, *Macromol. Rapid*

Commun., 2013, **34**, 1271-1283.

28. Z.-G. Wang and B. Ding, *Adv. Mater.*, 2013, **25**, 3905-3914.

29. T. Miyata, N. Asami and T. Uragami, *Nature*, 1999, **399**, 766-769.

30. G. Ye, C. Yang and X. Wang, *Macromol. Rapid Commun.*, 2010, **31**, 1332-1336.

31. R. Zhang, A. Bowyer, R. Eisenthal and J. Hubble, *Biotechnol. Bioeng.*, 2007, **97**, 976-984.

32. E. Kokufata, Y. Q. Zhang and T. Tanaka, *Nature*, 1991, **351**, 302-304.

33. L. R. Balaoing, A. D. Post, A. Y. Lin, H. Tseng, J. L. Moake and K. J. Grande-Allen, *Plos One*, 2015, **10**.

34. C. Wang, R. J. Stewart and J. Kopecek, *Nature*, 1999, **397**, 417-420.

35. M. Ikeda, T. Tanida, T. Yoshii, K. Kurotani, S. Onogi, K. Urayama and I. Hamachi, *Nat. Chem.*, 2014, **6**, 511-518.

36. X. Wang, D. Niu, P. Li, Q. Wu, X. Bo, B. Liu, S. Bao, T. Su, H. Xu and Q. Wang, *ACS nano*, 2015, **9**, 5646-5656.

37. Z. Yu, Q. Xu, C. Dong, S. S. Lee, L. Gao, Y. Li, M. D'Ortenzio and J. Wu, *Curr. Pharm. Des.*, 2015, **21**, 4342-4354.

38. J. D. Watson and F. H. C. Crick, *Nature*, 1953, **171**, 737-738.

39. E. Stulz, G. Clever, M. Shionoya and C. Mao, *Chem. Soc. Rev.*, 2011, **40**, 5633-5635.

40. N. C. Seeman, *Nature*, 2003, **421**, 427-431.

41. J. Marmur and P. Doty, *J. Mol. Biol.*, 1961, **3**, 585-594.

42. J. Choi, S. Kim, T. Tachikawa, M. Fujitsuka and T. Majima, *J. Am. Chem. Soc.*, 2011, **133**, 16146-16153.

43. M. Kuwahara and N. Sugimoto, *Molecules*, 2010, **15**, 5423-5444.

44. S. Nagahara and T. Matsuda, *Polym. Gels Networks*, 1996, **4**, 111-127.

45. L. Peng, C. S. Wu, M. You, D. Han, Y. Chen, T. Fu, M. Ye and W. Tan, *Chem. Sci.*, 2013, **4**, 1928-1938.

46. J. Liu, *Soft Matter.*, 2011, **7**, 6757.

47. J. Liu, H. Liu, H. Kang, M. Donovan, Z. Zhu and W. Tan, *Anal. Bioanal. Chem.*, 2012, **402**, 187-194.

48. D. Yang, M. R. Hartman, T. L. Derrien, S. Hamada, D. An, K. G. Yancey, R. Cheng, M. Ma and D. Luo, *Acc. Chem. Res.*, 2014, **47**, 1902-1911.

49. E. Mastronardi, A. Foster, X. Zhang and M. C. DeRosa, *Sensors*, 2014, **14**,

3156-3171.

50. J. L. MacLean, K. Morishita and J. Liu, *Biosens. Bioelectron.*, 2013, **48**, 82-86.

51. C. Goncalves, P. Pereira and M. Gama, *Materials*, 2010, **3**, 1420-1460.

52. Z. Zhang, S. Li, N. Chen, C. Yang and Y. Wang, *Biomacromolecules*, 2013, **14**, 1174-1180.

53. J. Song, K. Im, S. Hwang, J. Hur, J. Nam, G. O. Ahn, S. Hwang, S. Kim and N. Park, *Nanoscale*, 2015, **7**, 9433-9437.

54. T. Tokatlian, C. Cam and T. Segura, *Biomaterials*, 2014, **35**, 825-835.

55. S. H. Nezhadi, P. F. M. Choong, F. Lotfipour and C. R. Dass, *J. Drug Target.*, 2009, **17**, 731-738.

56. D. Costa, A. J. M. Valente, M. Graca Miguel and J. Queiroz, *Adv. Colloid. Interface Sci.*, 2014, **205**, 257-264.

57. F. E. Alemdaroglu and A. Herrmann, *Org. Biomol. Chem.*, 2007, **5**, 1311-1320.

58. H. J. Moon, D. Y. Ko, M. H. Park, M. K. Joo and B. Jeong, *Chem. Soc. Rev.*, 2012, **41**, 4860-4883.

59. F. D. Jochum and P. Theato, *Chem. Soc. Rev.*, 2013, **42**, 7468-7483.

60. B. Jeong, S. W. Kim and Y. H. Bae, *Adv. Drug Delivery Rev.*, 2002, **54**, 37-51.

61. H. G. Schild, *Prog. Polym. Sci.*, 1992, **17**, 163-249.

62. J. Ramos, A. Imaz and J. Forcada, *Polym. Chem.*, 2012, **3**, 852-856.

63. W. Guo, C.-H. Lu, X.-J. Qi, R. Orbach, M. Fadeev, H.-H. Yang and I. Willner, *Angew. Chem. Int. Ed.*, 2014, **53**, 10134-10138.

64. H. Kang, H. Liu, X. Zhang, J. Yan, Z. Zhu, L. Peng, H. Yang, Y. Kim and W. Tan, *Langmuir*, 2011, **27**, 399-408.

65. J. K. Lee, Y. H. Jung, J. B. H. Tok and Z. Bao, *ACS nano*, 2011, **5**, 2067-2074.

66. A. Rajendran, M. Endo, Y. Katsuda, K. Hidaka and H. Sugiyama, *J. Am. Chem. Soc.*, 2011, **133**, 14488-14491.

67. J. K. Lee, Y. H. Jung, R. M. Stoltenberg, J. B. H. Tok and Z. Bao, *J. Am. Chem. Soc.*, 2008, **130**, 12854-12855.

68. G. D. Cimino, H. B. Gamper, S. T. Isaacs and J. E. Hearst, *Annu. Rev. Biochem.*, 1985, **54**, 1151-1193.

69. M. R. Hartman, D. Yang, T. N. N. Tran, K. Lee, J. S. Kahn, P. Kiatwuthinon, K. G. Yancey, O. Trotsenko, S. Minko and D. Luo, *Angew. Chem. Int. Ed.*, 2013, **52**, 8699-8702.

70. Y. Xu, Q. Wu, Y. Sun, H. Bai and G. Shi, *ACS nano*, 2010, **4**, 7358-7362.

71. E. Cheng, Y. Li, Z. Yang, Z. Deng and D. Liu, *Chem. Commun.*, 2011, **47**, 5545-5547.

72. M. Shin, J. H. Ryu, J. P. Park, K. Kim, J. W. Yang and H. Lee, *Adv. Funct. Mater.*, 2015, **25**, 1270-1278.

73. K. T. Chung, T. Y. Wong, C. I. Wei, Y. W. Huang and Y. Lin, *Crit. Rev. Food Sci.*, 1998, **38**, 421-464.

74. S. H. Um, J. B. Lee, N. Park, S. Y. Kwon, C. C. Umbach and D. Luo, *Nat. Mater.*, 2006, **5**, 797-801.

75. N. Park, S. H. Um, H. Funabashi, J. Xu and D. Luo, *Nat. Mater.*, 2009, **8**, 432-437.

76. J. B. Lee, S. Peng, D. Yang, Y. H. Roh, H. Funabashi, N. Park, E. J. Rice, L. Chen, R. Long, M. Wu and D. Luo, *Nat. Nanotechnol.*, 2012, **7**, 816-820.

77. H. Qi, M. Ghodousi, Y. Du, C. Grun, H. Bae, P. Yin and A. Khademhosseini, *Nat. Commun.*, 2013, **4**, 2275.

78. E. Cheng, Y. Xing, P. Chen, Y. Yang, Y. Sun, D. Zhou, L. Xu, Q. Fan and D. Liu, *Angew. Chem.*, 2009, **121**, 7796-7799.

79. M. R. Jones, N. C. Seeman and C. A. Mirkin, *Science*, 2015, **347**, 6224.

80. H. Yan, S. H. Park, G. Finkelstein, J. H. Reif and T. H. LaBean, *Science*, 2003, **301**, 1882-1884.

81. P. W. K. Rothemund, *Nature*, 2006, **440**, 297-302.

82. R. P. Goodman, M. Heilemann, S. Doose, C. M. Erben, A. N. Kapanidis and A. J. Turberfield, *Nat. Nanotechnol.* , 2008, **3**, 93-96.

83. R. Schreiber, J. Do, E.-M. Roller, T. Zhang, V. J. Schueller, P. C. Nickels, J. Feldmann and T. Liedl, *Nat. Nanotechnol.*, 2014, **9**, 74-78.

84. Y. Zhang, F. Lu, K. G. Yager, D. van der Lelie and O. Gang, *Nat. Nanotechnol.*, 2013, **8**, 865-872.

85. L. Y. T. Chou, K. Zagorovsky and W. C. W. Chan, *Nat. Nanotechnol.*, 2014, **9**, 148-155.

86. V. M. Prabhu and S. D. Hudson, *Nat. Mater.*, 2009, **8**, 365-366.

87. Q. Yuan, Y. Zhang, Y. Chen, R. Wang, C. Du, E. Yasun and W. Tan, *Proc. Natl. Acad. Sci. U. S. A.*, 2011, **108**, 9331-9336.

88. N. C. Seeman, *Trends Biochem. Sci.*, 2005, **30**, 119-125.

89. J. Bath and A. J. Turberfield, *Nat. Nanotechnol.* , 2007, **2**, 275-284.

90. B. Yurke, A. J. Turberfield, A. P. Mills, F. C. Simmel and J. L. Neumann,

Nature, 2000, **406**, 605-608.

91. Y. Xing, E. Cheng, Y. Yang, P. Chen, T. Zhang, Y. Sun, Z. Yang and D. Liu, *Adv. Mater.*, 2011, **23**, 1117-1121.

92. A. J. Zaug and T. R. Cech, *Science*, 1986, **231**, 470-475.

93. C. Guerriertakada, K. Gardiner, T. Marsh, N. Pace and S. Altman, *Cell*, 1983, **35**, 849-857.

94. N. K. Vaish, A. W. Fraley, J. W. Szostak and L. W. McLaughlin, *Nucleic Acids Res.*, 2000, **28**, 3316-3322.

95. C. Teller and I. Willner, *Curr. Opin. Biotech.,* 2010, **21**, 376-391.

96. J. Liu, Z. Cao and Y. Lu, *Chem. Rev.* , 2009, **109**, 1948-1998.

97. T. Hermann and D. J. Patel, *J Mol. Biol.*, 1999, **294**, 829-849.

98. U. Nagaswamy, N. Voss, Z. D. Zhang and G. E. Fox, *Nucleic Acids Res.*, 2000, **28**, 375-376.

99. D. L. Robertson and G. F. Joyce, *Nature*, 1990, **344**, 467-468.

100. A. D. Ellington and J. W. Szostak, *Nature*, 1990, **346**, 818-822.

101. C. Tuerk and L. Gold, *Science*, 1990, **249**, 505-510.

102. M. Sassanfar and J. W. Szostak, *Nature*, 1993, **364**, 550-553.

103. R. D. Jenison, S. C. Gill, A. Pardi and B. Polisky, *Science*, 1994, **263**, 1425-1429.

104. A. A. Haller and P. Sarnow, *Proc. Natl. Acad. Sci. U. S. A.*, 1997, **94**, 8521-8526.

105. D. Shangguan, Y. Li, Z. Tang, Z. C. Cao, H. W. Chen, P. Mallikaratchy, K. Sefah, C. J. Yang and W. Tan, *Proc. Natl. Acad. Sci. U. S. A.*, 2006, **103**, 11838-11843.

106. Z. Tang, D. Shangguan, K. Wang, H. Shi, K. Sefah, P. Mallikratchy, H. W. Chen, Y. Li and W. Tan, *Anal. Chem.*, 2007, **79**, 4900-4907.

107. M. Rajendran and A. D. Ellington, *Anal. Bioanal.Chem.*, 2008, **390**, 1067-1075.

108. E. J. Cho, J.-W. Lee and A. D. Ellington, *Annu. Rev. Anal. Chem.*, 2009, **2**, 241-264.

109. J. R. Babendure, S. R. Adams and R. Y. Tsien, *J. Am. Chem. Soc.*, 2003, **125**, 14716-14717.

110. I. Willner and M. Zayats, *Angew. Chem. Int. Ed.*, 2007, **46**, 6408-6418.

111. J. Sargent, *Nat. Rev. Endocrinol.*, 2015, **11**, 194-194.

112. K. Sefah, J. A. Phillips, X. Xiong, L. Meng, D. Van Simaeys, H. Chen, J.

Martin and W. Tan, *Analyst*, 2009, **134**, 1765-1775.

113. T. Mairal, V. C. Oezalp, P. L. Sanchez, M. Mir, I. Katakis and C. K. O'Sullivan, *Anal. Bioanal. Chem.*, 2008, **390**, 989-1007.

114. E. N. Brody and L. Gold, *J. Biotechnol.*, 2000, **74**, 5-13.

115. L. Yang, X. Zhang, M. Ye, J. Jiang, R. Yang, T. Fu, Y. Chen, K. Wang, C. Liu and W. Tan, *Adv. Drug Delivery Rev.*, 2011, **63**, 1361-1370.

116. Q. Liu, C. Jin, Y. Wang, X. Fang, X. Zhang, Z. Chen and W. Tan, *NPG Asia Mater.*, 2014, **6**.

117. H. Yang, H. Liu, H. Kang and W. Tan, *J. Am. Chem. Soc.*, 2008, **130**, 6320-6321.

118. D. Liu, E. Cheng and Z. Yang, *NPG Asia Mater.*, 2011, **3**, 109-114.

119. F. El-Hamed, N. Dave and J. Liu, *Nanotechnology*, 2011, **22**.

120. C. Y. Hui, Y. Li and J. D. Brennan, *Chem. Mater.*, 2014, **26**, 1896-1904.

121. Z. Zhu, C. Wu, H. Liu, Y. Zou, X. Zhang, H. Kang, C. J. Yang and W. Tan, *Angew. Chem. Int. Ed.*, 2010, **49**, 1052-1056.

122. L. Yan, Z. Zhu, Y. Zou, Y. Huang, D. Liu, S. Jia, D. Xu, M. Wu, Y. Zhou, S. Zhou and C. J. Yang, *J. Am. Chem. Soc.*, 2013, **135**, 3748-3751.

123. Z. Zhu, Z. Guan, S. Jia, Z. Lei, S. Lin, H. Zhang, Y. Ma, Z. Q. Tian and C. J. Yang, *Angew. Chem. Int. Ed.*, 2014, **53**, 12503-12507.

124. L. Feng, Z. Lyu, A. Offenhaeusser and D. Mayer, *Angew. Chem. Int. Ed.*, 2015, **54**, 7693-7697.

125. M. Zhou, Y. Du, C. Chen, B. Li, D. Wen, S. Dong and E. Wang, *J. Am. Chem. Soc.*, 2010, **132**, 2172-2174.

126. L. Wang, J. Zhu, L. Han, L. Jin, C. Zhu, E. Wang and S. Dong, *ACS nano*, 2012, **6**, 6659-6666.

127. B. C. Yin, B. C. Ye, H. Wang, Z. Zhu and W. Tan, *Chem. Commun.*, 2012, **48**, 1248-1250.

128. L. Zhang, J. Lei, L. Liu, C. Li and H. Ju, *Anal. Chem.*, 2013, **85**, 11077-11082.

129. X. Wang and X. Wang, *Chem. Commun.,* 2013, **49**, 5957-5959.

130. R. L. Srinivas, S. C. Chapin and P. S. Doyle, *Anal. Chem.*, 2011, **83**, 9138-9145.

131. T.-H. Fan, B. Soontornworajit, M. Karzar-Jeddi, X. Zhang and Y. Wang, *Soft Matter.*, 2011, **7**, 9326-9334.

132. W. Bai, N. A. Gariano and D. A. Spivak, *J. Am. Chem. Soc.*, 2013, **135**,

6977-6984.

133. W. Bai and D. A. Spivak, *Angew. Chem. Int. Ed.*, 2014, **53**, 2095-2098.

134. R. Wang and Y. Li, *Biosens. Bioelectron.*, 2013, **42**, 148-155.

135. R. Langer, *Nature*, 1998, **392**, 5-10.

136. S. D. Putney and P. A. Burke, *Nat. Biotechnol.*, 1998, **16**, 153-157.

137. B. V. Slaughter, S. S. Khurshid, O. Z. Fisher, A. Khademhosseini and N. A. Peppas, *Adv. Mater.*, 2009, **21**, 3307-3329.

138. P. Andrade-Vivero, E. Fernandez-Gabriel, C. Alvarez-Lorenzo and A. Concheiro, *J. Pharm. Sci.*, 2007, **96**, 802-813.

139. N. S. Satarkar, D. Biswal and J. Z. Hilt, *Soft Matter.*, 2010, **6**, 2364-2371.

140. M. Hamidi, A. Azadi and P. Rafiei, *Adv. Drug Delivery Rev.*, 2008, **60**, 1638-1649.

141. B. Soontornworajit, J. Zhou, M. T. Shaw, T. H. Fan and Y. Wang, *Chem. Commun.*, 2010, **46**, 1857-1859.

142. B. Wei, I. Cheng, K. Q. Luo and Y. Mi, *Angew. Chem. Int. Ed.*, 2008, **47**, 331-333.

143. B. Soontornworajit, J. Zhou and Y. Wang, *Soft Matter.*, 2010, **6**, 4255.

144. X. He, B. Wei and Y. Mi, *Chem. Commun.*, 2010, **46**, 6308-6310.

145. B. Soontornworajit, J. Zhou, Z. Zhang and Y. Wang, *Biomacromolecules*, 2010, **11**, 2724-2730.

146. B. Soontornworajit, J. Zhou, M. P. Snipes, M. R. Battig and Y. Wang, *Biomaterials*, 2011, **32**, 6839-6849.

147. M. R. Battig, Y. Huang, N. Chen and Y. Wang, *Biomaterials*, 2014, **35**, 8040-8048.

148. M. R. Battig, B. Soontornworajit and Y. Wang, *J. Am. Chem. Soc.*, 2012, **134**, 12410-12413.

149. A. Shastri, L. M. McGregor, Y. Liu, V. Harris, H. Nan, M. Mujica, Y. Vasquez, A. Bhattacharya, Y. Ma, M. Aizenberg, O. Kuksenok, A. C. Balazs, J. Aizenberg and X. He, *Nat. Chem.*, 2015, **7**, 447-454.

150. N. Chen, Z. Zhang, B. Soontornworajit, J. Zhou and Y. Wang, *Biomaterials*, 2012, **33**, 1353-1362.

151. S. Li, N. Chen, Z. Zhang and Y. Wang, *Biomaterials*, 2013, **34**, 460-469.

152. Z. Zhang, N. Chen, S. Li, M. R. Battig and Y. Wang, *J. Am. Chem. Soc.,* 2012, **134**, 15716-15719.

153. E. R. Gaddes, G. Gydush, S. Li, N. Chen, C. Dong and Y. Wang, *Biomacromolecules*, 2015, **16**, 1382-1389.

154. E. Richards, S. Li, N. Chen, M. R. Battig and Y. Wang, *Biomacromolecules*, 2014, **15**, 4561-4569.

155. S. Li, E. R. Gaddes, N. Chen and Y. Wang, *Angew. Chem. Int. Ed.*, 2015, **54**, 5957-5961.

156. T. Chen, M. I. Shukoor, Y. Chen, Q. Yuan, Z. Zhu, Z. Zhao, B. Gulbakan and W. Tan, *Nanoscale*, 2011, **3**, 546-556.

157. Y. Zhong, F. Meng, C. Deng and Z. Zhong, *Biomacromolecules*, 2014, **15**, 1955-1969.

158. H. Kang, A. C. Trondoli, G. Zhu, Y. Chen, Y. J. Chang, H. Liu, Y. F. Huang, X. Zhang and W. Tan, *ACS nano*, 2011, **5**, 5094-5099.

159. G. Zhu, R. Hu, Z. Zhao, Z. Chen, X. Zhang and W. Tan, *J. Am. Chem. Soc.*, 2013, **135**, 16438-16445.

160. H.-M. Meng, X. Zhang, Y. Lv, Z. Zhao, N.-N. Wang, T. Fu, H. Fan, H. Liang, L. Qiu, G. Zhu and W. Tan, *ACS nano*, 2014, **8**, 6171-6181.

161. G. Zhu, J. Zheng, E. Song, M. Donovan, K. Zhang, C. Liu and W. Tan, *Proc. Natl. Acad. Sci. U. S. A.*, 2013, **110**, 7998-8003.

162. C. Wu, D. Han, T. Chen, L. Peng, G. Zhu, M. You, L. Qiu, K. Sefah, X. Zhang and W. Tan, *J. Am. Chem. Soc.*, 2013, **135**, 18644-18650.

163. J. Li, C. Zheng, S. Cansiz, C. Wu, J. Xu, C. Cui, Y. Liu, W. Hou, Y. Wang, L. Zhang, I. T. Teng, H. H. Yang and W. Tan, *J. Am. Chem. Soc.*, 2015, **137**, 1412-1415.

164. A. J. Zaug and T. R. Cech, *Cell*, 1980, **19**, 331-338.

165. K. Kruger, P. J. Grabowski, A. J. Zaug, J. Sands, D. E. Gottschling and T. R. Cech, *Cell*, 1982, **31**, 147-157.

166. E. A. Doherty and J. A. Doudna, *Annu. Rev. Biochem.*, 2000, **69**, 597-615.

167. J. A. Doudna and T. R. Cech, *Nature*, 2002, **418**, 222-228.

168. J. A. Doudna and J. R. Lorsch, *Nat. Struct. Mol. Biol.*, 2005, **12**, 395-402.

169. W. Pan and G. A. Clawson, *Expert. Opin. Biol. Ther.*, 2008, **8**, 1071-1085.

170. R. R. Breaker and G. F. Joyce, *Chem. Biol.*, 1994, **1**, 223-229.

171. P. Travascio, Y. Li and D. Sen, *Chem. Biol.*, 1998, **5**, 505-517.

172. R. R. Breaker and G. F. Joyce, *Chem. Biol.*, 1995, **2**, 655-660.

173. J. Liu and Y. Lu, *J. Am. Chem. Soc.*, 2007, **129**, 9838- 9839.

174. J. Liu and Y. Lu, *Angew. Chem. Int. Ed.*, 2007, **46**, 7587-7590.

175. M. Hollenstein, C. Hipolito, C. Lam, D. Dietrich and D. M. Perrin, *Angew. Chem. Int. Ed.*, 2008, **47**, 4346-4350.

176. J. Li, W. C. Zheng, A. H. Kwon and Y. Lu, *Nucleic Acids Res.*, 2000, **28**, 481-488.

177. A. Peracchi, *J Biol. Chem.*, 2000, **275**, 11693-11697.

178. J. Li and Y. Lu, *J. Am. Chem. Soc.*, 2000, **122**, 10466-10467.

179. J. Liu, A. K. Brown, X. Meng, D. M. Cropek, J. D. Istok, D. B. Watson and Y. Lu, *Proc. Natl. Acad. Sci. U. S. A.*, 2007, **104**, 2056-2061.

180. A. Roth and R. R. Breaker, *Proc. Natl. Acad. Sci. U. S. A.*, 1998, **95**, 6027-6031.

181. T. Pan and O. C. Uhlenbeck, *Nature*, 1992, **358**, 560-563.

182. S. Tsukiji, S. B. Pattnaik and H. Suga, *Nat. Struct. Biol.*, 2003, **10**, 713-717.

183. J. J. Agresti, B. T. Kelly, A. Jaschke and A. D. Griffiths, *Proc. Natl. Acad. Sci. U. S. A.*, 2005, **102**, 16170-16175.

184. L. Gong, Z. Zhao, Y.-F. Lv, S.-Y. Huan, T. Fu, X.-B. Zhang, G.-L. Shen and R.-Q. Yu, *Chem. Commun.*, 2015, **51**, 979-995.

185. J. W. Liu and Y. Lu, *J. Am. Chem. Soc.*, 2003, **125**, 6642-6643.

186. X.-B. Zhang, R.-M. Kong and Y. Lu, *Annu. Rev. Anal. Chem. (Palo Alto Calif),* 2011*,* **4***,* 105-128.

187. I. Willner, B. Shlyahovsky, M. Zayats and B. Willner, *Chem. Soc. Rev.*, 2008, **37**, 1153-1165.

188. S. Bi, Y. Yan, S. Hao and S. Zhang, *Angew. Chem. Int. Ed.*, 2010, **49**, 4438-4442.

189. Y. Chen and C. D. Mao, *J. Am. Chem. Soc.*, 2004, **126**, 8626-8627.

190. Y. Tian, Y. He, Y. Chen, P. Yin and C. D. Mao, *Angew. Chem. Int. Ed.*, 2005, **44**, 4355-4358.

191. F. Wang, C.-H. Lu and I. Willner, *Chem. Rev.* , 2014, **114**, 2881-2941.

192. P. Travascio, P. K. Witting, A. G. Mauk and D. Sen, *J. Am. Chem. Soc.*, 2001, **123**, 1337-1348.

193. V. Pavlov, Y. Xiao, R. Gill, A. Dishon, M. Kotler and I. Willner, *Anal. Chem.*, 2004, **76**, 2152-2156.

194. C. H. Lu, X. J. Qi, R. Orbach, H. H. Yang, I. Mironi-Harpaz, D. Seliktar and I. Willner, *Nano lett.*, 2013, **13**, 1298-1302.

195. H. Lin, Y. Zou, Y. Huang, J. Chen, W. Y. Zhang, Z. Zhuang, G. Jenkins and C. J.

Yang, *Chem. Commun.*, 2011, **47**, 9312-9314.

196. Y. Huang, Y. Ma, Y. Chen, X. Wu, L. Fang, Z. Zhu and C. J. Yang, *Anal. Chem.*, 2014, **86**, 11434-11439.

197. S. Lilienthal, Z. Shpilt, F. Wang, R. Orbach and I. Willner, *ACS Appl. Mater. Interfaces.*, 2015, **7**, 8923-8931.

198. Z. Yang, D. Hutter, P. Sheng, A. M. Sismour and S. A. Benner, *Nucleic Acids Res.*, 2006, **34**, 6095-6101.

199. K. Tanaka, G. H. Clever, Y. Takezawa, Y. Yamada, C. Kaul, M. Shionoya and T. Carell, *Nat. Nanotechnol.*, 2006, **1**, 190-U195.

200. E. Meggers, P. L. Holland, W. B. Tolman, F. E. Romesberg and P. G. Schultz, *J. Am. Chem. Soc.*, 2000, **122**, 10714-10715.

201. Y. Takezawa and M. Shionoya, *Acc. Chem. Res.* , 2012, **45**, 2066-2076.

202. G. H. Clever and M. Shionoya, *Coord. Chem. Rev.* 2010, **254**, 2391-2402.

203. M. Shionoya and K. Tanaka, *Curr. Opin. Chem. Biol.*, 2004, **8**, 592-597.

204. H. A. Wagenknecht, *Angew. Chem. Int. Ed.*, 2003, **42**, 3204-3206.

205. Y. Miyake, H. Togashi, M. Tashiro, H. Yamaguchi, S. Oda, M. Kudo, Y. Tanaka, Y. Kondo, R. Sawa, T. Fujimoto, T. Machinami and A. Ono, *J. Am. Chem. Soc.*, 2006, **128**, 2172-2173.

206. H. Urata, E. Yamaguchi, T. Funai, Y. Matsumura and S.-i. Wada, *Angew. Chem. Int. Ed.*, 2010, **49**, 6516-6519.

207. H. Yamaguchi, J. Sebera, J. Kondo, S. Oda, T. Komuro, T. Kawamura, T. Dairaku, Y. Kondo, I. Okamoto, A. Ono, J. V. Burda, C. Kojima, V. Sychrovsky and Y. Tanaka, *Nucleic Acids Res.*, 2014, **42**, 4094-4099.

208. F.-A. Polonius and J. Mueller, *Angew. Chem. Int. Ed.*, 2007, **46**, 5602-5604.

209. K. Tanaka, Y. Yamada and M. Shionoya, *J. Am. Chem. Soc.*, 2002, **124**, 8802-8803.

210. W. Deng, H. Xu, W. Ding and H. Liang, *Plos One*, 2014, **9**.

211. N. Dave, M. Y. Chan, P. J. Huang, B. D. Smith and J. Liu, *J. Am. Chem. Soc.*, 2010, **132**, 12668-12673.

212. K. A. Joseph, N. Dave and J. Liu, *ACS Appl. Mater. Interfaces.*, 2011, **3**, 733-739.

213. Y. Helwa, N. Dave, R. Froidevaux, A. Samadi and J. Liu, *ACS Appl. Mater. Interfaces.*, 2012, **4**, 2228-2233.

214. B.-F. Ye, Y.-J. Zhao, Y. Cheng, T.-T. Li, Z.-Y. Xie, X.-W. Zhao and Z.-Z. Gu,

Nanoscale, 2012, **4**, 5998-6003.

215. Y. Wang, M. Guo, X. Zheng, Q. Tang and D. Gao, *Prog. Chem.*, 2007, **19**, 1475-1480.

216. M. Chen, Y. Zhang, S. Jia, L. Zhou, Y. Guan and Y. Zhang, *Angew. Chem. Int. Ed.*, 2015, **54**, 9257-9261.

217. Z. Cai, N. L. Smith, J.-T. Zhang and S. A. Asher, *Anal. Chem.* , 2015, **87**, 5013-5025.

218. W. Guo, X. J. Qi, R. Orbach, C. H. Lu, L. Freage, I. Mironi-Harpaz, D. Seliktar, H. H. Yang and I. Willner, *Chem. Commun.*, 2014, **50**, 4065-4068.

219. W. Guo, R. Orbach, I. Mironi-Harpaz, D. Seliktar and I. Willner, *Small*, 2013, **9**, 3748-3752.

220. H. A. Day, P. Pavlou and Z. A. E. Waller, *Bioorg. Med. Chem.*, 2014, **22**, 4407-4418.

221. K. Gehring, J. L. Leroy and M. Gueron, *Nature*, 1993, **363**, 561-565.

222. Y. Dong, Z. Yang and D. Liu, *Acc. Chem. Res.*, 2014, **47**, 1853-1860.

223. W. Guo, C. H. Lu, R. Orbach, F. Wang, X. J. Qi, A. Cecconello, D. Seliktar and I. Willner, *Adv. Mater.*, 2015, **27**, 73-78.

224. R. S. Geary, D. Norris, R. Yu and C. F. Bennett, *Adv. Drug Delivery Rev.*, 2015, **87**, 46-51.

225. P. Boisguerin, S. Deshayes, M. J. Gait, L. O'Donovan, C. Godfrey, C. A. Betts, M. J. A. Wood and B. Lebleu, *Adv. Drug Delivery Rev.*, 2015, **87**, 52-67.

226. G. J. Hannon, *Nature*, 2002, **418**, 244-251.

227. M. L. Stephenson and P. C. Zamecnik, *Proc. Natl. Acad. Sci. U. S. A.*, 1978, **75**, 285-288.

228. P. C. Zamecnik and M. L. Stephenson, *Proc. Natl. Acad. Sci. U. S. A.*, 1978, **75**, 280-284.

229. D. P. Bartel, *Cell*, 2004, **116**, 281-297.

230. D. P. Bartel, *Cell*, 2009, **136**, 215-233.

231. R. W. Carthew and E. J. Sontheimer, *Cell*, 2009, **136**, 642-655.

232. Y. Dorsett and T. Tuschl, *Nat. Rev. Drug Discov.*, 2004, **3**, 318-329.

233. A. Fire, S. Q. Xu, M. K. Montgomery, S. A. Kostas, S. E. Driver and C. C. Mello, *Nature*, 1998, **391**, 806-811.

234. A. P. McCaffrey, L. Meuse, T.-T. T. Pham, D. S. Conklin, G. J. Hannon and M. A. Kay, *Nature*, 2002, **418**, 38-39.

235. C. A. Hong, S. H. Lee, J. S. Kim, J. W. Park, K. H. Bae, H. Mok, T. G. Park and H. Lee, *J. Am. Chem. Soc.*, 2011, **133**, 13914-13917.

236. C. A. Hong, J. S. Kim, S. H. Lee, W. H. Kong, T. G. Park, H. Mok and Y. S. Nam, *Adv. Funct. Mater.*, 2013, **23**, 316-322.

237. A. M. Krieg, *Annu. Rev. Biochem.,* 2002, **20**, 709-760.

238. J. E. Wooldridge and G. J. Weiner, *Curr. Opin. Oncol.*, 2003, **15**, 440-445.

239. M. Nishikawa, Y. Mizuno, K. Mohri, N. Matsuoka, S. Rattanakiat, Y. Takahashi, H. Funabashi, D. Luo and Y. Takakura, *Biomaterials*, 2011, **32**, 488-494.

240. M. Nishikawa, K. Ogawa, Y. Umeki, K. Mohri, Y. Kawasaki, H. Watanabe, N. Takahashi, E. Kusuki, R. Takahashi, Y. Takahashi and Y. Takakura, *J. Control. Release*, 2014, **180**, 25-32.

Fig. 1 Hydrogel formation induced by hybrid formation of DNA. (A) Hydrogel (type I) via hybridization between (oligoT)-derivatized water-soluble copolymer with complementary oligoA; (B) Hydrogel (type II) via hybridization between oligoA and oligoT attached to the side chains of corresponding copolymers. Adapted with permission from ref. 44. Copyright (1996) Elsevier.

Fig. 2 Formation of Y-shaped DNA branches and DNA hydrogel by PCR. (A) Three single-stranded DNAs hybridize to form Y-shaped DNA branches through DNA base pairing. DNA branches are treated with psoralen to cause covalent interstrand crosslinking. Resulting structures are thermostable and will remain intact under denaturing conditions. (B) Formation of DNA hydrogel using Y-shaped DNA branches by PCR reaction. Adapted with permission from ref. 69. Copyright (2013) Wiley-VCH.

Fig. 3 Examples of pure DNA hydrogels. (A) Schematic diagram of branched DNA monomers (X-, Y- and T-DNA) that serve as crosslinkers to form networked hydrogels. Adapted with permission from ref. 74. Copyright (2006) Nature Publishing Group. (B) Schematic diagram of the stepwise approach for DNA hydrogel synthesis based on RCA and MCA processes. Adapted with permission from ref. 76. Copyright (2012) Nature Publishing Group. (C) The pH-responsive DNA hydrogel. DNA hydrogel made from the three-dimensional assembly of Y-shaped DNA using i-motif structure as the crosslinking element. Adapted with permission from ref. 78. Copyright (2009) Wiley-VCH. (D) Schematic representation of DNA hydrogel formation. The Y-scaffold and linker are designed to crosslink by hybridization of their sticky ends, and accumulating this hybridization will lead to hydrogel formation. Adapted with permission from ref. 91. Copyright (2011) Wiley-VCH.

Fig. 4 (A) Schematic illustration of a hydrogel crosslinked by DNA containing adenosine-binding aptamer as it undergoes gel-to-sol transition upon adding target adenosine. (B) Photograph of hydrogel having entrapped AuNPs without and with adenosine. (C) Absorption measurements of AuNPs in the hydrogel system upon addition of adenosine. Reprinted with the permission from ref. 117. Copyright (2008) American Chemical Society.

Fig. 5 Schematic illustration of the target-responsive "sweet" aptamer-based hydrogel. The hydrogel with trapped glucoamylase is formed by hybridization of the aptamer and its partially complementary DNA polymer strands (**S-4** and **S-5**). The aptamers specifically identify the target cocaine to form target-aptamer complexes, leading to breakdown of the hydrogel and release of glucoamylase, which catalyzes the hydrolysis of amylose to produce a large amount of glucose for quantitative readout by the glucometer. Reprinted with the permission from ref. 122. Copyright (2013) American Chemical Society.

Fig. 6 Schematic illustration of the Au@Pt NPs-encapsulated target-responsive hydrogel with a V-chip readout for visual quantitative detection. Reprinted with the permission from ref. 123. Copyright (2014) Wiley-VCH.

Fig. 7 The "AND" logic gate system based on aptamer-crosslinked hydrogel. The hydrogel dissociated only when both cocaine and ATP were present. Adapted with the

permission from ref. 127. Copyright (2012) Royal Society of Chemistry.

Fig. 8 Scheme of a hybrid microfluidic system for biomolecule capture-and-release. (A) pH-dependent reversible binding and releasing of thrombin by the DNA aptamer at pH=6-7 and pH < 5, respectively, caused by the change of aptamer configuration. (B) pH-dependent reversible volume change of hydrogel, which swells at pH > pKa = 4.3, when the carboxylic groups are deprotonated, leading to the absorption of water into the gel matrix, and contracts at pH < pKa = 4.3, leading to the expulsion of water. (C) A cross-sectional view of the biphasic microfluidic chamber under constant laminar flow with aptamer-decorated microstructures. Reprinted with permission from ref. 149. Copyright (2015) Nature Publishing Group.

Fig. 9 Schematic illustration demonstrating the use of a programmable hydrogel for cell capture-and-release. (A) Transformation of the aptamer. (B) Cell capture-and-release by strand displacement strategy. Hybridization with the primary CS enables the display of the aptamer for cell capture. The secondary CS competes against the primary CS to hybridize and release the aptamer from the hydrogel, resulting in cell release. Adapted with the permission from ref. 152. Copyright (2012) American Chemical Society.

Fig. 10 (A) Schematic illustration of structural changes during molecular reconfiguration. (B) Schematic illustration of the remodeling of the **S-13**-functionalized hydrogel during hybridization reactions. The function of the hydrogel is determined by the active and inert states of **S-14**, respectively. **S-14** is the unblocking sequence, and **S-15** is the recovering sequence. Adapted with the permission from ref. 155. Copyright (2015) Wiley-VCH.

Fig. 11 Schematic illustration of aptamer-functionalized core-shell nanohydrogels for targeted chemotherapy. Adapted with the permission from ref. 158. Copyright (2011) American Chemical Society.

Fig. 12 Schematic illustration of stimuli-responsive DNA nanohydrogel formation. The Y-shaped monomers (YMA and YMB) and linker (LK) are designed to crosslink by hybridization of their sticky end segments (black lines), leading to nanohydrogel formation. Adapted with the permission from ref. 163. Copyright (2015) American Chemical Society.

Fig. 13 (A) Schematic illustration of metallo-base pairs-based CPCHs for the detection of heavy metal ions. (B) Volume change of CPCHs after binding of Hg^{2+} ions. (C) Effect of Hg^{2+} concentration on the diffraction wavelength of CPCHs. Top: diffraction color changes from red to blue with increasing Hg^{2+} concentration. Reprinted with the permission from ref. 214. Copyright (2012) Royal Society of Chemistry.

Fig. 14 Schematic illustration of a pH-switchable, shape-memory DNA hydrogel. Synthesis of (**S-20**) and (**S-21**) DNA-functionalized acrylamide copolymer and their crosslinking at pH 5.0 is performed in the mold by the i-motif and duplex structure (**S-21**)/(**S-21**) to yield a triangular hydrogel structure. The separated hydrogel triangular structure is subjected to pH 8.0 to separate the i-motif bridges and yield an amorphous quasi-liquid state that includes the duplexes as bridging shape-memory elements. Changing pH to 5.0 recovers the triangle-shaped hydrogel. Adapted with the permission

from ref. 223. Copyright (2015) Wiley-VCH.

Fig. 15 Synthetic scheme for the preparation of multimeric siRNA (M-siRNA), moderately branched siRNA hydrogel (DY-siRNA) and highly branched siRNA hydrogel (DY-siRNA). Adapted with the permission from ref. 235. Copyright (2011) American Chemical Society.

TOC:

We survey advances in bioanalytical and biomedical applications of functional nucleic acid-based hydrogels in this review.

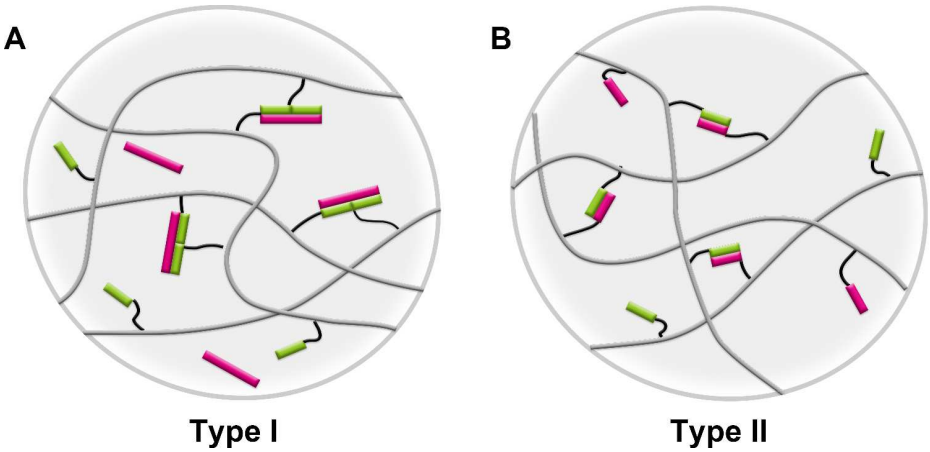

Fig. 1 Hydrogel formation induced by hybrid formation of DNA. (A) Hydrogel (type I) via hybridization between (oligoT)-derivatized water-soluble copolymer with complementary oligoA; (B) Hydrogel (type II) via hybridization between oligoA and oligoT attached to the side chains of corresponding copolymers. Adapted with permission from ref. 44. Copyright (1996) Elsevier.

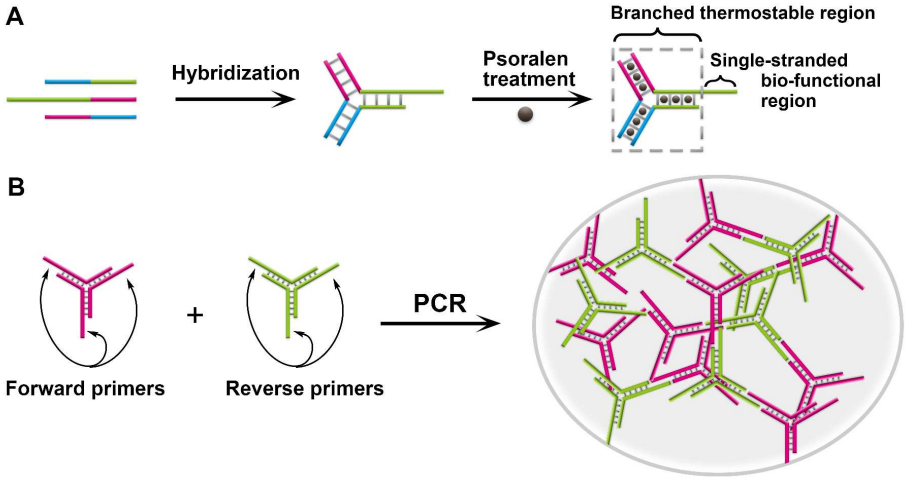

Fig. 2 Formation of Y-shaped DNA branches and DNA hydrogel by PCR. (A) Three single-stranded DNAs hybridize to form Y-shaped DNA branches through DNA base pairing. DNA branches are treated with psoralen to cause covalent interstrand crosslinking. Resulting structures are thermostable and will remain intact under denaturing conditions. (B) Formation of DNA hydrogel using Y-shaped DNA branches by PCR reaction. Adapted with permission from ref. 69. Copyright (2013) Wiley-VCH.

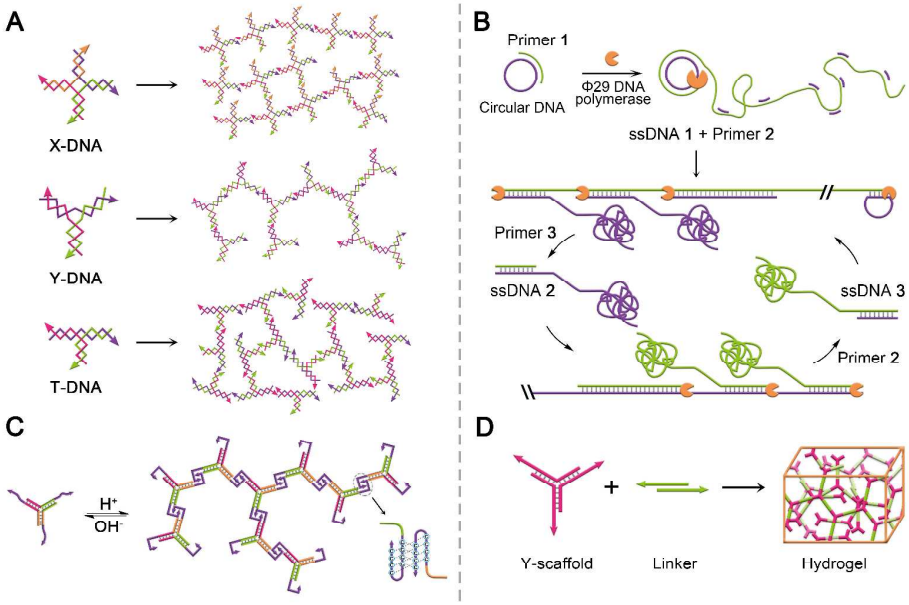

Fig. 3 Examples of pure DNA hydrogels. (A) Schematic diagram of branched DNA monomers (X-, Y- and T-DNA) that serve as crosslinkers to form networked hydrogels. Adapted with permission from ref. 74. Copyright (2006) Nature Publishing Group. (B) Schematic diagram of the stepwise approach for DNA hydrogel synthesis based on RCA and MCA processes. Adapted with permission from ref. 76. Copyright (2012) Nature Publishing Group. (C) The pH-responsive DNA hydrogel. DNA hydrogel made from the three-dimensional assembly of Y-shaped DNA using i-motif structure as the crosslinking element. Adapted with permission from ref. 78. Copyright (2009) Wiley-VCH. (D) Schematic representation of DNA hydrogel formation. The Y-scaffold and linker are designed to crosslink by hybridization of their sticky ends, and accumulating this hybridization will lead to hydrogel formation. Adapted with permission from ref. 91. Copyright (2011) Wiley-VCH.

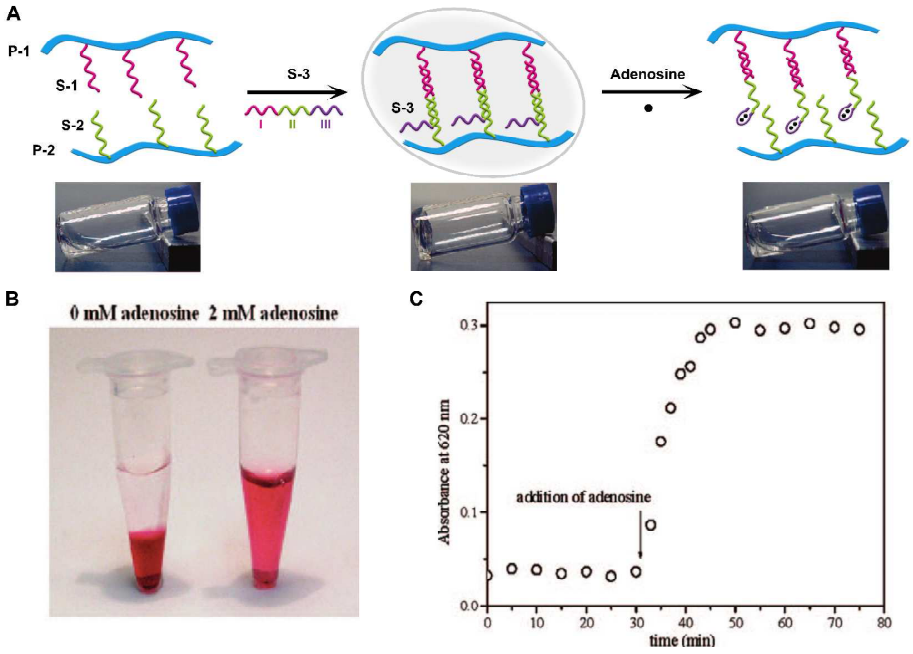

Fig. 4 (A) Schematic illustration of a hydrogel crosslinked by DNA containing adenosine-binding aptamer as it undergoes gel-to-sol transition upon adding target adenosine. (B) Photograph of hydrogel having entrapped AuNPs without and with adenosine. (C) Absorption measurements of AuNPs in the hydrogel system upon addition of adenosine. Reprinted with the permission from ref. 117. Copyright (2008) American Chemical Society.

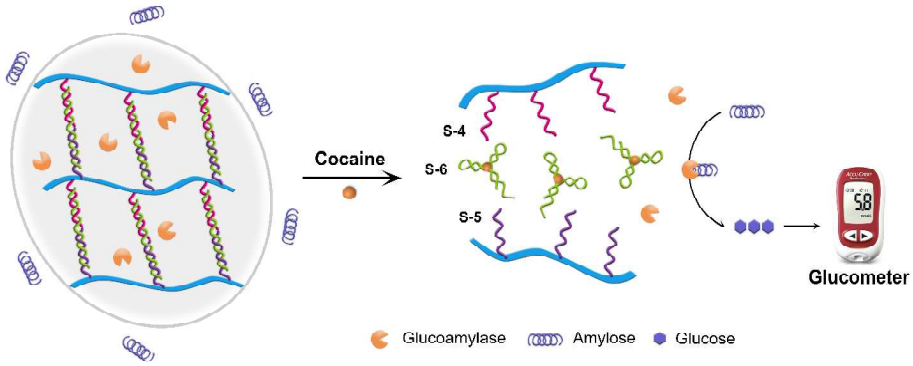

Fig. 5 Schematic illustration of the target-responsive "sweet" aptamer-based hydrogel. The hydrogel with trapped glucoamylase is formed by hybridization of the aptamer and its partially complementary DNA polymer strands (**S-4** and **S-5**). The aptamers specifically identify the target cocaine to form target-aptamer complexes, leading to breakdown of the hydrogel and release of glucoamylase, which catalyzes the hydrolysis of amylose to produce a large amount of glucose for quantitative readout by the glucometer. Reprinted with the permission from ref. 122. Copyright (2013) American Chemical Society.

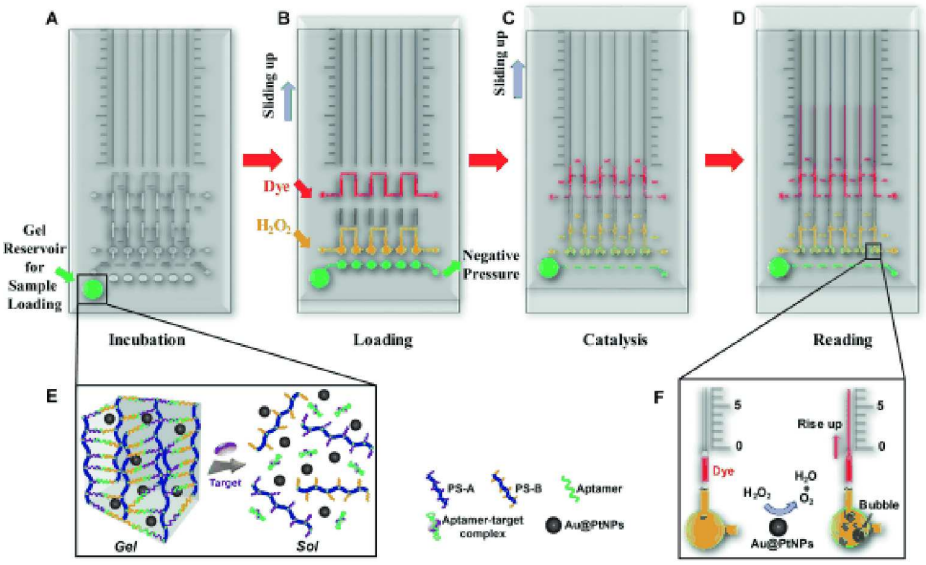

Fig. 6 Schematic illustration of the Au@Pt NPs-encapsulated target-responsive hydrogel with a V-chip readout for visual quantitative detection. Reprinted with the permission from ref. 123. Copyright (2014) Wiley-VCH.

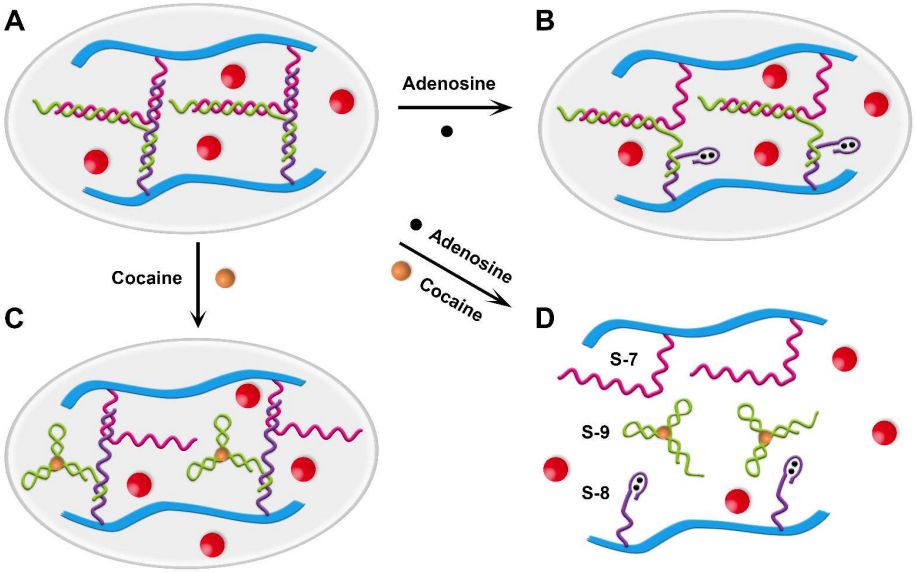

Fig. 7 The "AND" logic gate system based on aptamer-crosslinked hydrogel. The hydrogel dissociated only when both cocaine and ATP were present. Adapted with the permission from ref. 127. Copyright (2012) Royal Society of Chemistry.

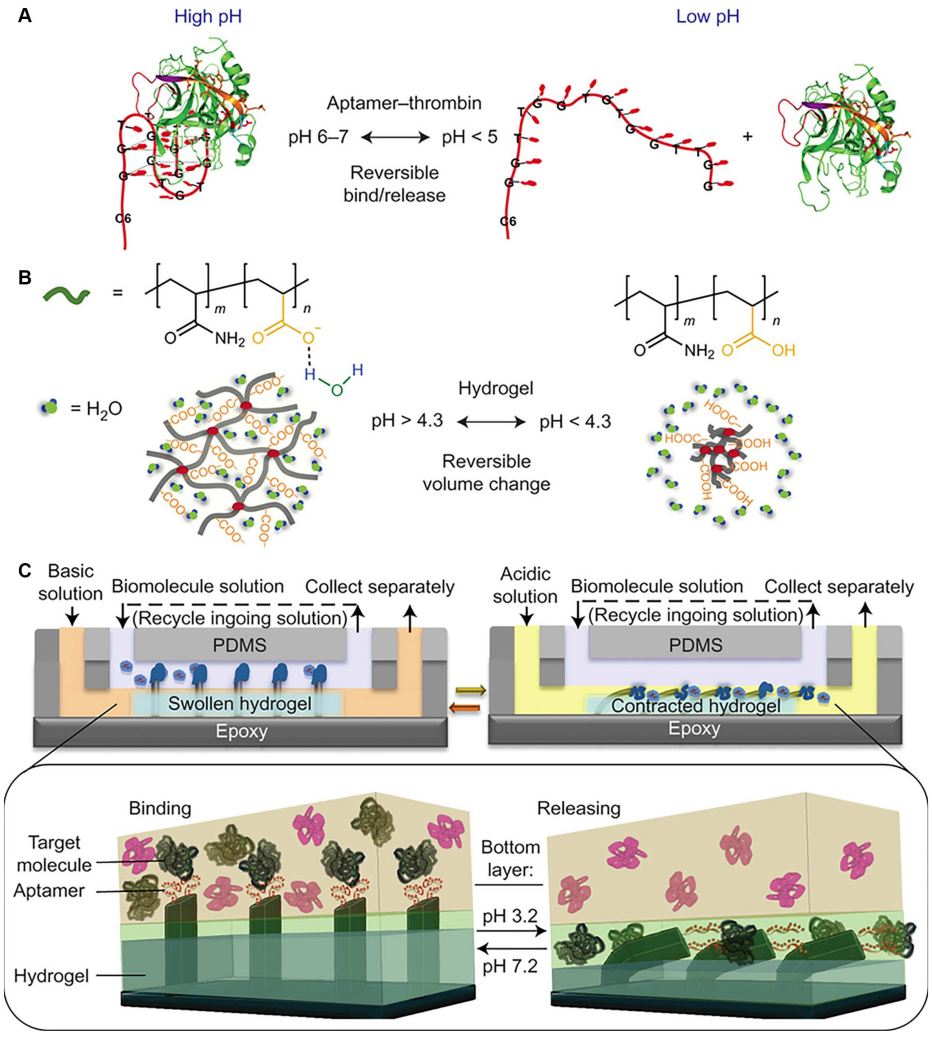

Fig. 8 Scheme of a hybrid microfluidic system for biomolecule capture-and-release. (A) pH-dependent reversible binding and releasing of thrombin by the DNA aptamer at pH=6-7 and pH < 5, respectively, caused by the change of aptamer configuration. (B) pH-dependent reversible volume change of hydrogel, which swells at pH > pKa = 4.3, when the carboxylic groups are deprotonated, leading to the absorption of water into the gel matrix, and contracts at pH < pKa = 4.3, leading to the expulsion of water. (C) A cross-sectional view of the biphasic microfluidic chamber under constant laminar flow with aptamer-decorated microstructures. Reprinted with permission from ref. 149. Copyright (2015) Nature Publishing Group.

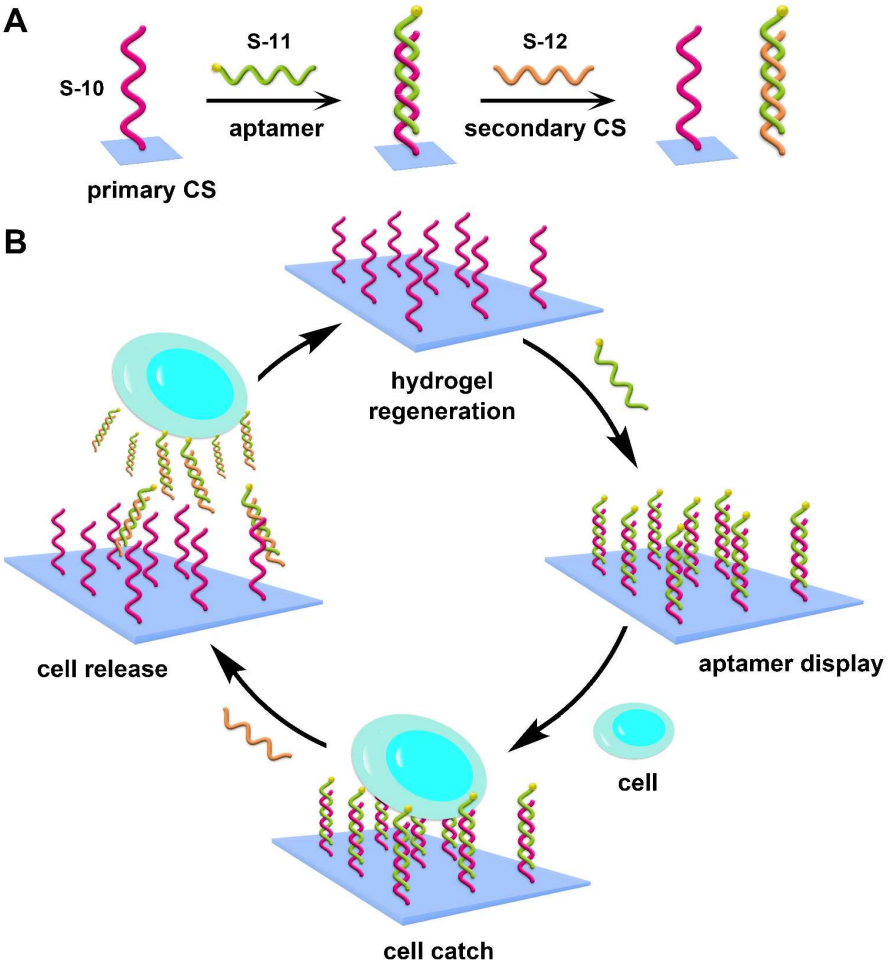

Fig. 9 Schematic illustration demonstrating the use of a programmable hydrogel for cell capture-and-release. (A) Transformation of the aptamer. (B) Cell capture-and-release by strand displacement strategy. Hybridization with the primary CS enables the display of the aptamer for cell capture. The secondary CS competes against the primary CS to hybridize and release the aptamer from the hydrogel, resulting in cell release. Adapted with the permission from ref. 152. Copyright (2012) American Chemical Society.

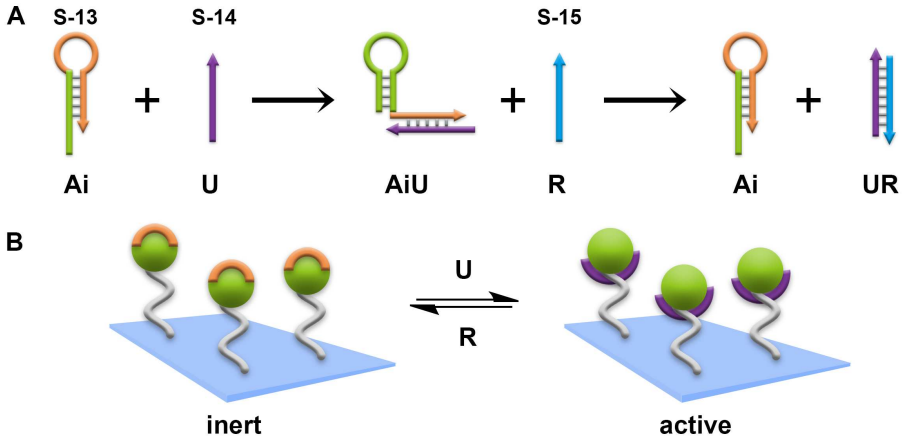

Fig. 10 (A) Schematic illustration of structural changes during molecular reconfiguration. (B) Schematic illustration of the remodeling of the **S-13**-functionalized hydrogel during hybridization reactions. The function of the hydrogel is determined by the active and inert states of **S-14**, respectively. **S-14** is the unblocking sequence, and **S-15** is the recovering sequence. Adapted with the permission from ref. 155. Copyright (2015) Wiley-VCH.

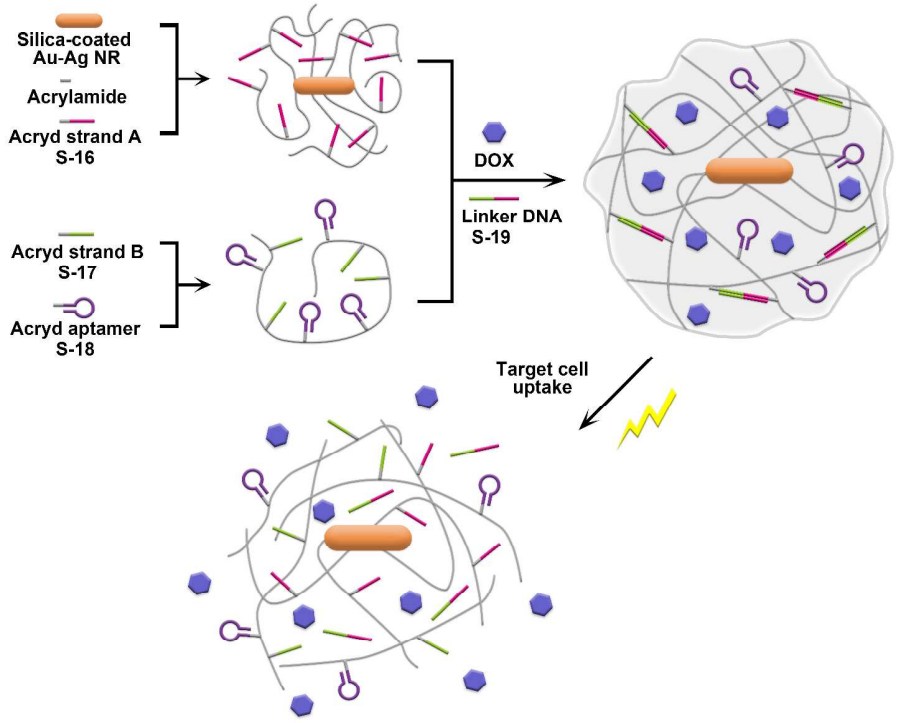

Fig. 11 Schematic illustration of aptamer-functionalized core-shell nanohydrogels for targeted chemotherapy. Adapted with the permission from ref. 158. Copyright (2011) American Chemical Society.

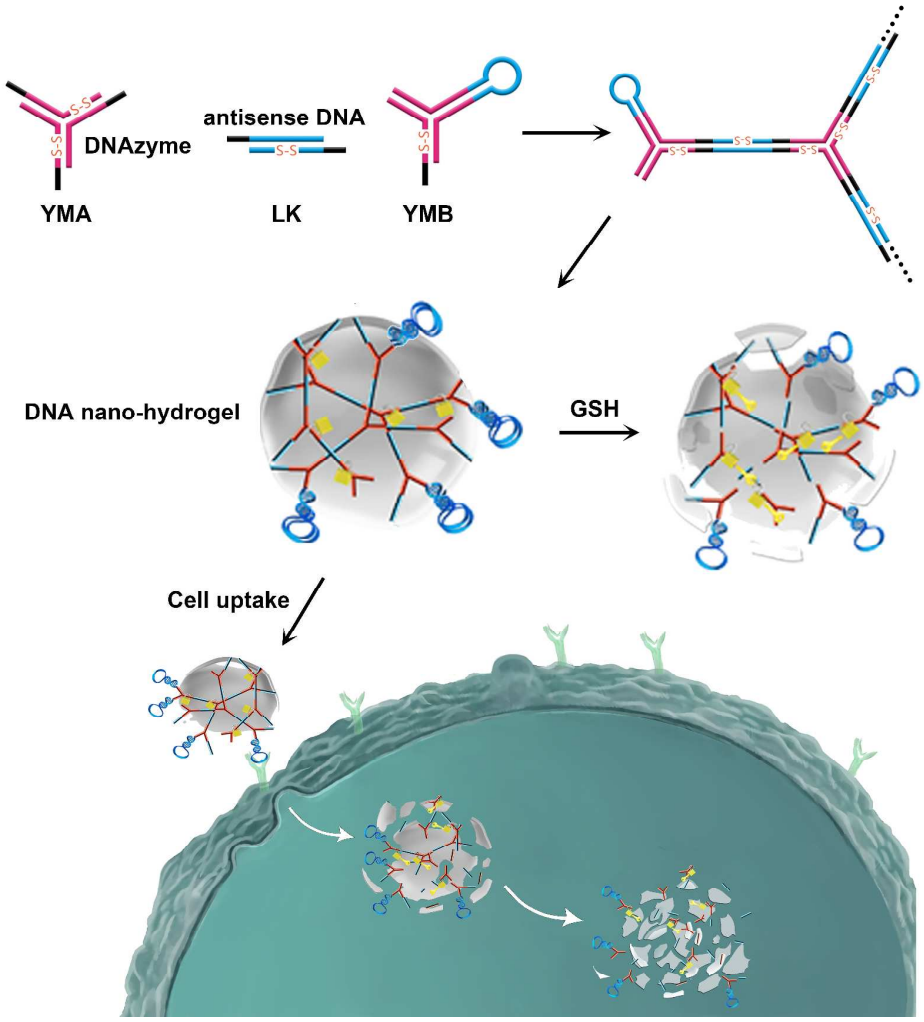

Fig. 12 Schematic illustration of stimuli-responsive DNA nanohydrogel formation. The Y-shaped monomers (YMA and YMB) and linker (LK) are designed to crosslink by hybridization of their sticky end segments (black lines), leading to nanohydrogel formation. Adapted with the permission from ref. 163. Copyright (2015) American Chemical Society.

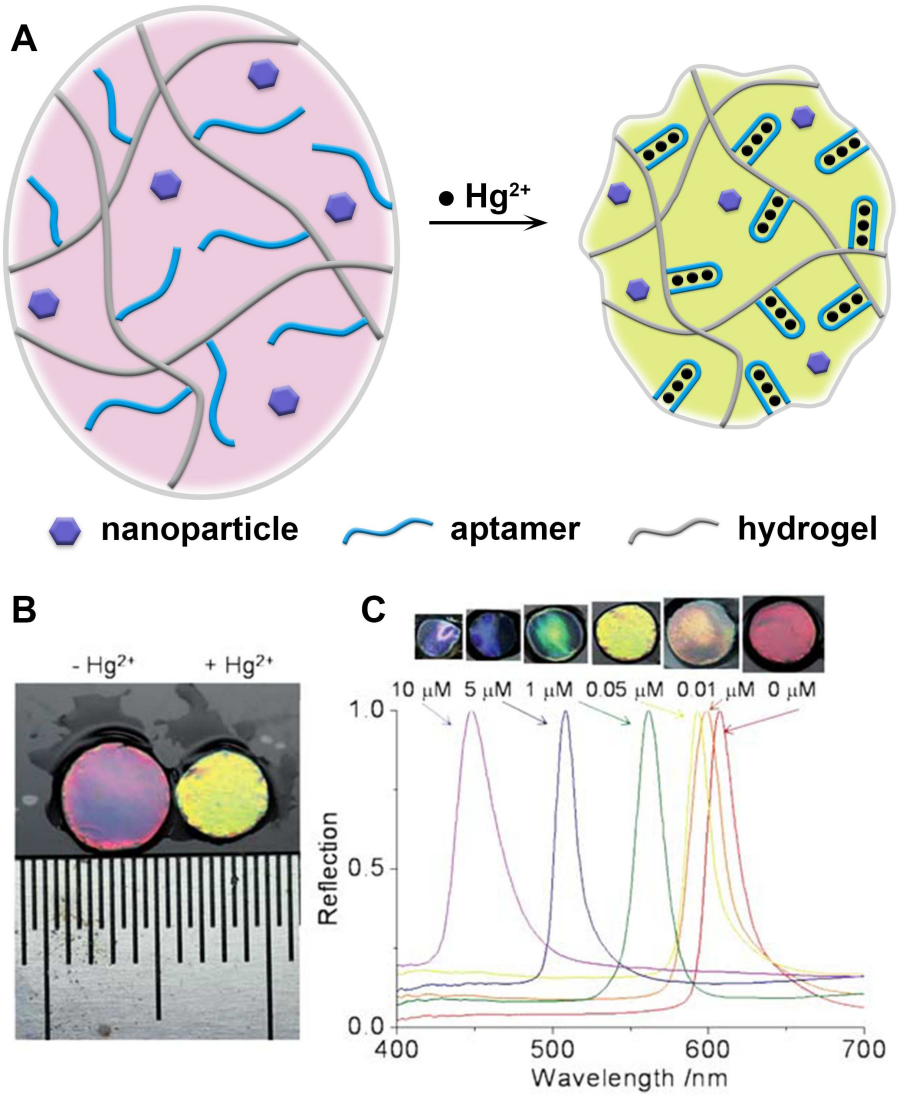

Fig. 13 (A) Schematic illustration of metallo-base pairs-based CPCHs for the detection of heavy metal ions. (B) Volume change of CPCHs after binding of Hg^{2+} ions. (C) Effect of Hg^{2+} concentration on the diffraction wavelength of CPCHs. Top: diffraction color changes from red to blue with increasing Hg^{2+} concentration. Reprinted with the permission from ref. 214. Copyright (2012) Royal Society of Chemistry.

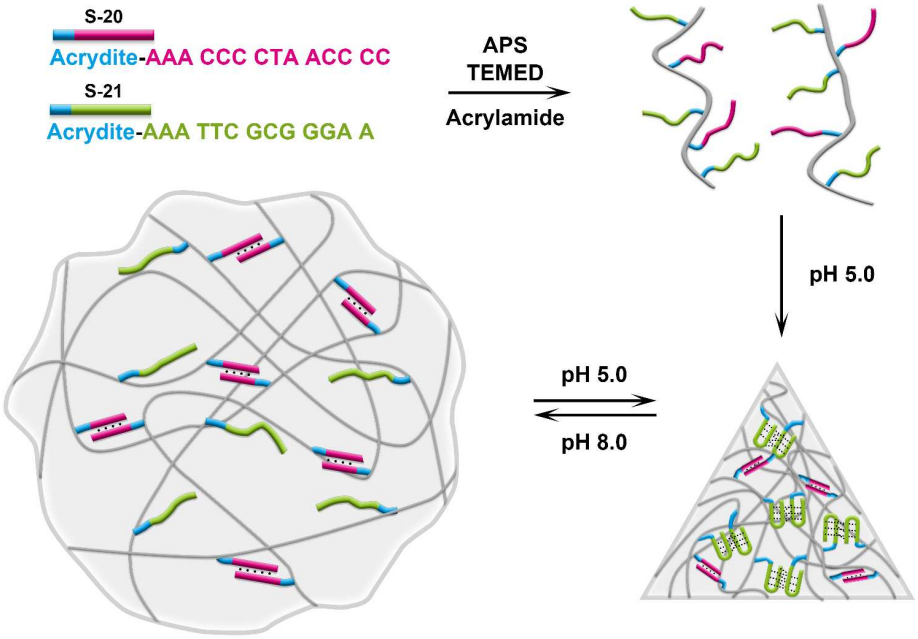

Fig. 14 Schematic illustration of a pH-switchable, shape-memory DNA hydrogel. Synthesis of (**S-20**) and (**S-21**) DNA-functionalized acrylamide copolymer and their crosslinking at pH 5.0 is performed in the mold by the i-motif and duplex structure (**S-21**)/(**S-21**) to yield a triangular hydrogel structure. The separated hydrogel triangular structure is subjected to pH 8.0 to separate the i-motif bridges and yield an amorphous quasi-liquid state that includes the duplexes as bridging shape-memory elements. Changing pH to 5.0 recovers the triangle-shaped hydrogel. Adapted with the permission from ref. 223. Copyright (2015) Wiley-VCH.

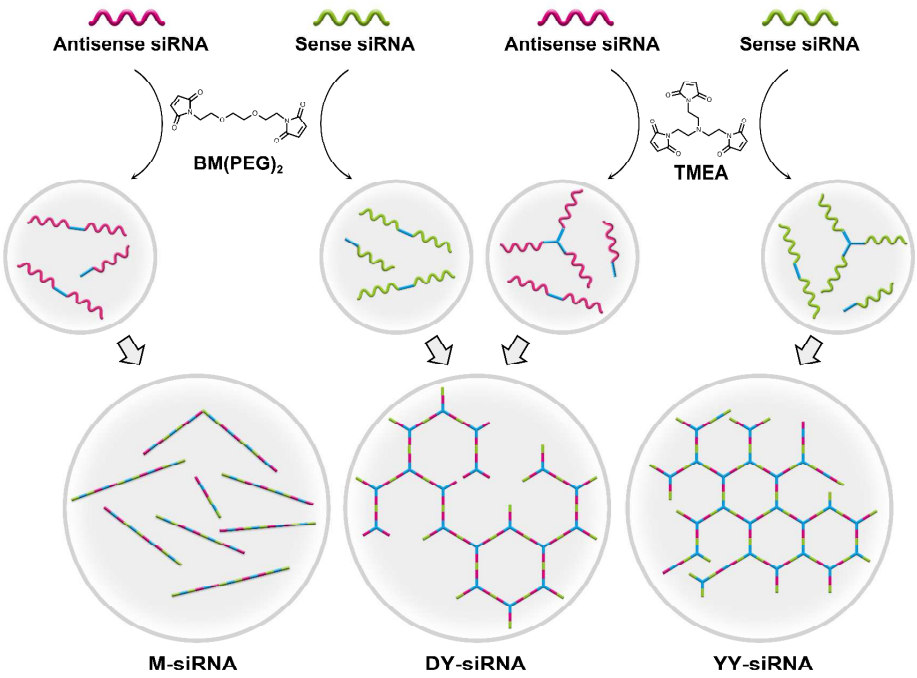

Fig. 15 Synthetic scheme for the preparation of multimeric siRNA (M-siRNA), moderately branched siRNA hydrogel (DY-siRNA) and highly branched siRNA hydrogel (DY-siRNA). Adapted with the permission from ref. 235. Copyright (2011) American Chemical Society.